Chemical-genetic interaction landscape of mono-(2-ethylhexyl)-phthalate using chemogenomic profiling in yeast

Mohammad Alfatah[1]*, Jin Huei Wong[1], Kiat Whye Kong[2], Felix Utama[3], Shawn Hoon[2], and Prakash Arumugam[1]*

1. Bioinformatics Institute, 30 Biopolis Street, #07-01, Matrix, Singapore 138671

2. Molecular Engineering Laboratory, 61 Biopolis Drive, #03-12 Proteos, Singapore 13867

3. School of Chemical and Life Sciences, Singapore Polytechnic, 500 Dover Road, Singapore 139651

*To whom correspondence must be addressed

Email: alfatahm@bii.a-star.edu and prakasha@bii.a-star.edu

Key Words

Mono-(2-ethylhexyl)-phthalate (MEHP); Di-(2-ethylhexyl)-phthalate (DEHP); Chemogenomic profiling; Chemical-genetic interaction; *Saccharomyces cerevisiae*

Abstract

Integration of chemical-genetic interaction data with biological functions provides a mechanistic understanding of how toxic compounds affect cells. Mono-(2-ethylhexyl)-phthalate (MEHP) is an active metabolite of di-(2-ethylhexyl)-phthalate (DEHP), a commonly used plasticizer. MEHP adversely affects human health causing hepatotoxicity and reproductive toxicity. How MEHP affects cellular physiology is not fully understood. We utilized a genome-wide competitive fitness-based assay called 'chemogenomic profiling' to determine the genetic interaction map of MEHP in *Saccharomyces cerevisiae.* Gene Ontology enrichment analysis of 218 genes that provide resistance to MEHP indicated that MEHP affects seven cellular processes namely: (1) cellular amino acid biosynthetic process, (2) sterol biosynthetic process (3) cellular transport, (4) transcriptional and translational regulation, (5) protein glycosylation, (6) cytokinesis and cell morphogenesis and (7) ionic homeostasis. We show that MEHP protects yeast cells from membrane perturbing agents such as amphotericin B, dihydrosphingosine and phytosphingosine. Moreover, we also demonstrate that MEHP compromises the integrity of the yeast plasma membrane and cell wall. Our work provides a basis for further investigation of MEHP toxicity in humans.

1. Introduction

Understanding how environmental factors affect cellular physiology and shape their survival and evolution is a fundamental question in biology. Environmental factors could be either natural or artificial with either beneficial or deleterious effects to cellular systems. For example, heavy metals are essential for cellular functions but at high doses they are toxic to cells (Tchounwou et al., 2012; Jaishankar et al., 2014). The detrimental effect is not only limited to heavy metals; nutrients, toxic chemicals and pharmaceutical drugs could also adversely affect cellular systems (Carpenter et al., 2002; Kola and Landis, 2004; Kramer et al., 2007). Genome-wide mapping of biological and molecular responses to environmental factors is important to understand the mechanism by which environmental factors perturb cellular physiology.

Phthalates constitute a class of widely distributed environmental factors that have the potential of adversely affecting human health (Heudorf et al., 2007; Kamrin, 2009; Braun et al., 2013; Serrano et al., 2014; Gao and Wen, 2016). Chemically, phthalates are esters of an aromatic dicarboxylic acid called phthalic acid (Cao, 2010). Phthalates cause a wide-range of deleterious effects including neurotoxicity, reproductive toxicity, skeletal anomalies, allergy, obesity and cancer (Heudorf et al., 2007; Kamrin, 2009; Braun et al., 2013; Benjamin et al., 2017; Stroustrup et al., 2018). They are most commonly used as plasticizers to improve several physical properties of plastics such as flexibility and stability (Cao, 2010; Serrano et al., 2014; Gao and Wen, 2016).

Among the phthalates, di-(2-ethylhexyl)-phthalate (DEHP) is the most widely used plasticizer (Rudel and Perovich, 2009; Halden, 2010; Rowdhwal and Chen, 2018) and is a well-known endocrine disrupting chemical (EDCs). World-wide annual production of DEHP is more than 2 million tons (Halden, 2010; Rowdhwal and Chen, 2018). It is abundantly used in a variety of applications ranging from food and beverage packaging to medical devices such as catheters, intravenous bags, dialysis bags and blood bags (Cao, 2010; Lioy et al., 2015; Benjamin et al., 2017; Rowdhwal and Chen, 2018). DEHP weakly binds to plastic polymer matrix *via* a non-covalent interaction. Therefore, it can get easily leached into the environment following treatment of plastics with surfactants and organic solvents resulting in their ubiquitous exposure to human population (Halden, 2010; Benjamin et al., 2017; Rowdhwal and Chen, 2018). Humans can get exposed to DEHP *via* its ingestion, inhalation and dermal contact (Heudorf et al., 2007; Kamrin, 2009; Braun et al., 2013; Gao and Wen, 2016; Benjamin et al., 2017). Following entry into the human body, DEHP is quickly converted by pancreatic lipase to mono-(2-ethylhexyl) phthalate (MEHP) which is preferentially absorbed and biologically active (Albro and Thomas, 1973; Saito et al., 2010). The ability of DEHP to disrupt endocrine function and cause various forms of toxicity is mainly mediated by MEHP (Kratochvil et al.; Rudel and Perovich, 2009; Rowdhwal and Chen, 2018).

How MEHP interacts with cellular systems and affects several physiological functions is not well understood. MEHP has been reported to cause oxidative stress, lipid peroxidation, DNA damage and inhibition of steroid production (Inada et al., 2012; Yang et al., 2012; Yao et al., 2012; Tetz et al., 2013; Sobarzo et al., 2015). Its ability to inhibit expression and activity of antioxidant enzymes has been proposed to cause the various adverse effects (Bonilla and del Mazo, 2010; Wang et al., 2012; Craig et

al., 2014). Lack of information about the genes which interact with MEHP has limited the understanding of its molecular interaction.

Chemogenomic profiling is a powerful approach to uncover the mode-of-action of chemicals in *Saccharomyces cerevisiae* (Giaever et al., 2004; Hoon et al., 2008; Hillenmeyer et al., 2010). By performing a competitive fitness-based assay with a defined library of mutants in the presence of a compound of interest, genes that confer sensitivity or resistance to the compound can be identified generating insights into its mode-of-action. There are three major kinds of chemogenomic profiling assays in yeast namely haploinsufficiency profiling (HIP), homozygous profiling (HOP) and multicopy suppression profiling (MSP). HIP identify direct targets and gene that act closely with targets genes in the cell. HOP identify pathways that buffer or act in parallel to the target gene function. Target genes which when over expressed confer resistance to a bioactive compound can be identified by MSP. We performed homozygous profiling in *Saccharomyces cerevisiae* to uncover the biological pathways and their related genes that provide resistance to MEHP-toxicity. Our work has unravelled a role for MEHP in several biological processes such as amino acid uptake, sterol biosynthesis, vesicular transport and ionic homeostasis. Our results are largely consistent with a recent genome-wide study of MEHP resistance in yeast (Jiang et al., 2018). We also show that MEHP disrupts the integrity of yeast plasma membrane and cell wall. As some components associated with tolerance to MEHP are evolutionarily conserved, our results provide a basis to uncover the mechanism of MEHP-induced toxicity in mammalian systems.

2. Materials and methods

2.1. Yeast strain, chemicals and growth conditions

Derivatives of the diploid *Saccharomyces cerevisiae* BY4743 strain were used in this study. Yeast strains were recovered from frozen glycerol stocks on yeast extract-peptone-dextrose (YPD) agar medium (1% Bacto yeast extract, 2% Bacto peptone, 2% glucose, and 2.5% Bacto agar). Yeast cells were grown in YPD broth at 30°C with shaking at 220 rpm. YPD-HEPES (YPD + 25 mM HEPES, pH=6.8) medium was used for the growth inhibitory assays. Stock solutions of Mono-(2-ethylhexyl)-phthalate (3.6M stock, Wako), Di-(2-ethylhexyl)-phthalate (2.5M stock, Sigma), Amphotericin B (5mM stock, Sigma), Dihydrosphingosine (32mM stock, Avanti lipid), Phytosphingosine (64mM stock, TCI chemicals) and Calcofluor White (10mg/ml stock, Sigma) were prepared in Dimethyl Sulfoxide (Sigma). Final concentration of DMSO did not exceed 2% in all the assays.

2.2. Inhibitory concentration determination

Inhibitory Concentration (IC) of DEHP and MEHP was determined for the *Saccharomyces cerevisiae* strain BY4743 Cells grown overnight in YPD broth were diluted to a starting OD_{600nm} of 0.0625 in YPD-HEPES (YPD + 25 mM HEPES, pH=6.8) medium. Cell suspension (200 µL) was transferred into a 96-well microtiter plate containing serially double-diluted concentrations of compound. Cells were incubated at 30°C with shaking at 220 rpm for 16 hours. IC of compound was calculated using GraphPad Prism 8 software by comparing the growth of treated-and untreated-cells. Curve was fitted by nonlinear regression using the replicate data of % growth relative to untreated control. The IC20 concentration of MEHP (2.3 mM) was used to perform the chemogenomic profiling assay.

2.3. Chemogenomic profiling

Chemogenomic profiling was performed using a pooled barcoded library of *S. cerevisiae* diploid homozygous deletion strains (Invitrogen). We included six biological replicates for the control DMSO-treated cells and two biological replicates for the MEHP-treated cells. Homozygous profiling (HOP) assay was performed described as previously (Ng et al., 2018; Alfatah et al., 2019). Briefly, frozen aliquots of pooled bar-coded deletion strains were treated with either DMSO or 2.3 mM MEHP at a starting OD_{600} of 0.0625 in YPD-HEPES (YPD + 25 mM HEPES, pH=6.8) medium and grown for 5 generations ($OD_{600nm} \leq 2$) with shaking (200 rpm) at 30°C. Cells were transferred to a microfuge tube and pelleted by centrifugation. Genomic DNA was isolated from cell pellets and used as a template to PCR amplify the uptag bar-code sequences of pooled strains. A forward primer containing an unique 6-bp TruSeq index sequence and a common reverse primer was used to amplify the uptag bar-code (Supplementary information). The purified PCR products were pooled and sequenced on an Illumina HiSeq 2500 platform. NGS data were deposited at the NCBI's Sequence Read Archive (SRA) database (accession: PRJNA522816).

2.4. Bioinformatics methods

Sequenced reads were demultiplexed raw fastq reads were processed in the following way. First, reads without the adaptor sequence (GTCCACGAGGTCTCT) flanking the uptag barcode were filtered out. The uptag barcodes were then extracted and identical sequences were then counted and collapsed. The TAG counts were then aligned to a library of known TAG sequences to link each read count to the deletion strain using the Novoalign software (http://novocraft.com V2.05.33) with the default settings (-n 22 to truncate the reads to the length of the tag barcode). This setting allowed up to a

single base pair mismatch. The SAM files generated were parsed and the total counts of each TAG corresponding to each homozygous deletion strain were tabulated. These counts were then analyzed with the EdgeR analysis package (Robinson et al., 2010) using the generalized linear model (glm) mode to contrast the treated samples to the control (DMSO) sample and differentially sensitive strains were identified. We used the generalized linear models (glm) and estimated the trended and tagwise dispersion using the *estimatedGLMTrendedDisp* and *estimateGLMTagwiseDisp* functionality. A likelihood ratio test was then used (glmFIT() and glmLRT()) to test for differential expression. This provided a log fold-change ratio of tags between treated and control samples. A threshold value of $p<0.05$ was used to identify mutants with significant growth defect which were chosen for further analysis. Gene Ontology (GO) analysis was performed using the online tools DAVID (Huang da et al., 2009b, a) and GO terms that had p-value <0.05 were analysed by REVIGO (Supek et al., 2011).

2.5. Checkerboard growth assay

Cell growth in the presence of two different compounds was performed by checkerboard broth microdilution assay (Haque et al., 2016). Two-fold dilutions of the two compounds used in each experiment were prepared and dispensed into a 96-well microtiter plate. Cells grown in YPD medium were diluted to OD_{600nm} of 0.0625 in media (YPD + 25mM HEPES, pH 6.8). Cell suspension was distributed in microtiter plate (200 µl/well) and incubated at 30°C with 220 rpm shaking for 24 hours. To assess the interaction between two compounds, synergy was calculated using the Bliss independence model. The Bliss model is commonly employed in evaluation of synergism which is based on the assumption that compounds act independently and do not interfere with each other (Stathias et al., 2018). Bliss plots were generated using

the web application SynergyFinder [https://synergyfinder.fimm.fi] (Ianevski et al., 2017).

2.6. Propidium Iodide (PI) and Calcofluor White (CFW) staining

Cells grown in YPD medium were diluted to OD_{600nm}≈0.5 in YPD-HEPES (YPD + 25 mM HEPES, pH=6.8) medium and incubated with MEHP or DEHP or DMSO for 4 hours. For PI staining, cells were washed twice and resuspended in PBS and incubated with 5 µg/ml PI for 20 min in the dark with shaking at 25°C. For CFW staining, cultures were fixed with 4% paraformaldehyde for 30 min with shaking at 30°C. Cells were then washed twice and resuspended in PBS with 20 µg/ml CFW and incubated for 30 min in the dark with shaking at 25°C. Following staining, cells were washed and resuspended in PBS. Cells were directly visualized by bright-field and fluorescence microscope using a 100X objective lens. Excitation/Emission wavelengths of PI and CFW were 535 nm /617 nm and 365 nm/435 nm respectively. Percentage of PI or CFW stained cells (N≥100) was calculated.

3. Results

3.1. Chemogenomic profiling analysis

Saccharomyces cerevisiae is an excellent system to determine mode-of-action of compounds as about 33% of its genes have human homologues. We first tested the effect of DEHP and its biologically active derivative MEHP on the growth of the yeast strain BY4743. MEHP completely inhibited the growth of BY4743 cells at 9 mM (Fig. 1A). In contrast, DEHP had no effect on growth of yeast cells even at 25 mM (Supplementary Fig. S1B). Thus, the relative inhibitory effects of MEHP and DEHP

241 on yeast and mammalian cells is conserved indicating that mechanistic insights into
242 MEHP's toxicity could be obtained from further investigations in yeast.
243
244 To characterize the MEHP-genetic interaction, we performed Homozygous profiling (
245 HOP), a genome-wide fitness-based assay that can identify genes that confer either
246 resistance or sensitivity to a compound in a single experiment (Giaever et al., 2004;
247 Hoon et al., 2008; Hillenmeyer et al., 2010). Results from a genome-wide sensitivity
248 screening using individual deletion strains of non-essential genes onto YPD plates
249 supplemented with MEHP were recently reported (Jiang et al., 2018). We used MEHP
250 at IC_{20} concentration (2.3 mM) for the chemogenomic profiling assay. We grew the
251 pooled barcoded library of yeast deletion strains in the presence of either MEHP or
252 DMSO for about 5 generations. We used the genomic DNA from the two cultures as
253 a template to PCR amplify the barcodes and determined their sequences by NGS. The
254 relative proportion of 4817 deletion strain in the two cultures was used to calculate
255 their Fitness Coefficient (FC) (Supplementary table. 1). The logFC was plotted against
256 P-value (Fig. 1B). MEHP-sensitive and MEHP-resistant strains are expected to have
257 negative and positive logFC values respectively. Most of the 4817 deletion strains had
258 logFC values close to 0 but there were some which had a significantly high positive or
259 a negative value. We validated HOP data by testing individually growth of 14 top hit
260 mutants which were either sensitive (9 mutants) or resistant to MEHP (5 mutants). All
261 the 9 mutants with negative logFC values were sensitive to MEHP in comparison to
262 the wild type strain confirming the HOP data (Fig. 1C). However, none of the 5 mutants
263 with positive logFC scores were resistant to MEHP (Fig. 1C). Therefore, we focused
264 on the MEHP-sensitive mutants for further study.
265

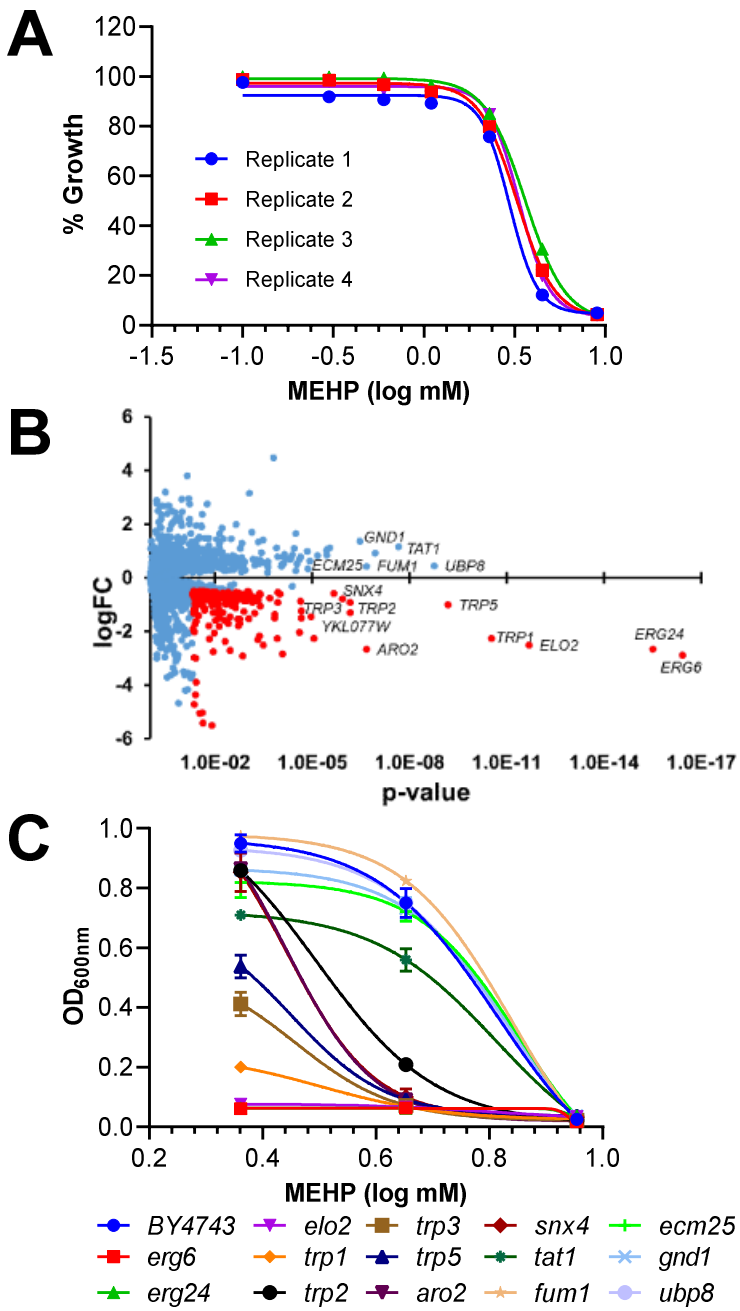

Fig. 1. Chemogenomic profiling of MEHP in *Saccharomyces cerevisiae*.

A. Inhibitory Concentration (IC) of MEHP was determined for *Saccharomyces cerevisiae* strain (BY4743). Cells were incubated with various concentrations MEHP in YPD-HEPES (YPD + 25 mM HEPES, pH=6.8) medium at 30°C. Experiments were performed with four replicates in 96-well microplate. Growth of the cells was quantified

by measuring the OD_{600nm} after 16 hours. Growth is plotted against concentration of the compound.

B. Fitness Coefficient (logFC) was plotted against P-value for the 4817 deletion mutants that were analyzed by homozygous profiling (HOP) assay. logFC negative value of a mutant indicates sensitive to MEHP. Mutants that have logFC<-0.5 and p-value <0.05 are shown by red dots and the remaining are indicated as blue dots. For the clear visualization, gene names of only 15 top hits are indicated in the plot.

C. Wild type strain BY4743 and 15 deletion strains that were sensitive to MEHP in the HOP assay, were grown in the YPD-HEPES (YPD + 25 mM HEPES, pH=6.8) medium in the presence of different concentrations of MEHP. Growth at the different concentrations of MEHP tested after 24 hours of incubation at 30°C is plotted for each strain. Representative data from two biological replicates are shown in the figure.

3.2. MEHP-genetic interaction and functional classification

To gain insights into MEHP's mode of action, we performed Gene Ontology (GO) analysis of 218 genes that provide resistance to MEHP using the online tool DAVID (Huang da et al., 2009b, a). We chose genes whose deletions had logFC<-0.5 and P-value <0.05 (Supplementary table. 1). Many of the GO terms under biological process were redundant under different annotation clusters (total number is 28) (Supplementary table. 1). We removed the redundant GO terms using the online tool REVIGO (Supek et al., 2011); and visualized their corresponding biological functions (Fig. 2). We classified the genetic interactions into the following seven categories (Table. 1) based on related biological functions; (1) cellular amino acid biosynthetic process, (2) sterol biosynthetic process (3) cellular transport, (4) transcriptional and translational regulation, (5) protein glycosylation, (6) cytokinesis and cell

morphogenesis and (7) ionic homeostasis. Similar MEHP-genetic interaction maps was found by a recent study (Jiang et al., 2018). We further studied the top three functional categories to understand their biological and molecular responses in a cellular context. A total of 12 genes belong to the first functional category “cellular amino acid biosynthetic process”. *TRP1, TRP2, TRP3, TRP4, TRP5* and *MET8, MET10, MET14* encode enzymes involved in the biosynthesis of tryptophan and methionine amino acids respectively. In addition, genes such as *ARO2* (chorismate metabolic process), *GCN4* (bZIP transcriptional activator of amino acid biosynthetic genes), *ABZ1* (synthesis of para-aminobenzoic acid) and *PUT1* (utilization of proline as sole nitrogen source) were in the same functional category. Five genes were in the second functional category “steroid biosynthetic process” (*ERG24, ERG4, ERG5, ERG6, ATG26*). *ERG* genes are involved in biosynthesis of membrane sterol (ergosterol in yeast and cholesterol in higher eukaryotes). *ATG26* encodes a conserved UDP-glucose:sterol glucosyltransferase involved in synthesis of sterol glucoside membrane lipids. The functional category “cellular transport” contains total 18 genes *(SYS1, CLC1, SSH1, VPS3, SNX4, MON2, APS3, SEC66, GET2, NUP60, VID24, PEP8, GET1, APL5, YPT52, VPS16, VPS21, VPS36).* These genes are mainly involved in intracellular protein transport, vesicle-mediated transport, endosomal transport and vacuolar transport (equivalent to lysosomal transport in humans). “Cellular Component” enrichment analysis indicated that several gene products were localized to the plasma membrane part (GO:0044459, 12 genes), plasma membrane (GO:0005886, 21 genes) and internal side of plasma membrane (GO:0009898, 9 genes) (Supplementary table. 1). “Molecular Function” enrichment analysis showed that some of the MEHP-resistance gene products were phosphoinositide binding (GO:0035091, 5 genes), phospholipid binding (GO:0005543, 5 genes) and lipid

binding (GO:0008289, 5 genes) (Supplementary table. 1). Taken together, our results suggest that MEHP exacerbates the growth defect of deletion strains impaired in amino acid biosynthesis, ergosterol biosynthesis and cellular transport.

Fig. 2. Genetic interaction mapping of MEHP in *Saccharomyces cerevisiae*. Enrichment of biological process GO terms among the top 218 genes conferring resistance (logFC value <-0.5 and P-value <0.05) to MEHP was determined by using online tool DAVID and redundant GO terms were removed by online tool REVIGO. The plot shows the enrichment of biological process associated with MEHP. The semantic similarities between the non-redundant GO terms are represented as scatterplots in 2-dimensional space. Related GO terms cluster together in the plot. The p-value for the false discovery rates of each GO term is represented by the colour of

the corresponding circle. The GO term frequency in the GO database is represented by the size of the corresponding circle.

Table. 1

MEHP-genetic interaction functional categories.

Functional category	**GO term_ID**	**Description**
1. Cellular amino acid biosynthetic process	GO:0000162	tryptophan biosynthetic process
	GO:0042401	cellular biogenic amine biosynthetic process
	GO:0006576	cellular biogenic amine metabolic process
	GO:0006568	tryptophan metabolic process
	GO:0046219	indolalkylamine biosynthetic process
	GO:0006586	indolalkylamine metabolic process
	GO:0042435	indole-containing compound biosynthetic process
	GO:0009073	aromatic amino acid family biosynthetic process
	GO:0009309	amine biosynthetic process
	GO:0042430	indole-containing compound metabolic process
	GO:0006575	cellular modified amino acid metabolic process
	GO:0042398	cellular modified amino acid biosynthetic process
	GO:0046417	chorismate metabolic process
	GO:0043648	dicarboxylic acid metabolic process
	GO:0008652	cellular amino acid biosynthetic process
	GO:0016053	organic acid biosynthetic process
	GO:0046394	carboxylic acid biosynthetic process
	GO:0009086	methionine biosynthetic process
	GO:0006555	methionine metabolic process
	GO:0000097	sulfur amino acid biosynthetic process
	GO:0009067	aspartate family amino acid biosynthetic process
	GO:0000096	sulfur amino acid metabolic process
	GO:0000103	sulfate assimilation
2. Sterol biosynthetic process	GO:0006694	steroid biosynthetic process
	GO:0016129	phytosteroid biosynthetic process

	GO:0016125	sterol metabolic process
	GO:0016126	sterol biosynthetic process
	GO:0016128	phytosteroid metabolic process
	GO:0006696	ergosterol biosynthetic process
	GO:0008204	ergosterol metabolic process
3. Cellular transport	GO:0006886	intracellular protein transport
	GO:0070727	cellular macromolecule localization
	GO:0034613	cellular protein localization
	GO:0006887	exocytosis
	GO:0032940	secretion by cell
	GO:0046903	secretion
4. Transcriptional and translational regulation	GO:0006366	transcription from RNA polymerase II promoter
	GO:0010528	regulation of transposition
	GO:0006351	transcription, DNA-templated
	GO:0032774	RNA biosynthetic process
	GO:0006417	regulation of translation
	GO:0010529	negative regulation of transposition
	GO:0010525	regulation of transposition, RNA-mediated
	GO:0010526	negative regulation of transposition, RNA-mediated
5. Protein glycosylation	GO:0070085	glycosylation
	GO:0006486	protein glycosylation
	GO:0009101	glycoprotein biosynthetic process
	GO:0043413	macromolecule glycosylation
	GO:0009100	glycoprotein metabolic process
6. Cytokinesis and cell morphogenesis	GO:0000910	cytokinesis
	GO:0007105	cytokinesis, site selection
	GO:0000282	cellular bud site selection
	GO:0007163	establishment or maintenance of cell polarity
	GO:0000902	cell morphogenesis
	GO:0032989	cellular component morphogenesis
	GO:0030029	actin filament-based process
	GO:0030036	actin cytoskeleton organization
7. Ionic homeostasis	GO:0045851	pH reduction
	GO:0051453	regulation of intracellular pH
	GO:0030004	cellular monovalent inorganic cation homeostasis
	GO:0051452	intracellular pH reduction
	GO:0030641	regulation of cellular pH
	GO:0007035	vacuolar acidification
	GO:0006885	regulation of pH
	GO:0055067	monovalent inorganic cation homeostasis

3.3. Addition of tryptophan to the medium rescues the MEHP-sensitivity of *trp* mutants

Chemogenomic profiling revealed a genetic interaction between MEHP and tryptophan biosynthetic gene deletions (*trp1Δ*, *trp2 Δ*, *trp3Δ*, *trp4Δ* and *trp5Δ*). We first confirmed that all the 5 mutants were sensitive to MEHP as compared to wild type strains (Fig. 3A) but not to DEHP (Supplementary Fig. S1B). The *trp* mutants are dependent on uptake of tryptophan from the medium. If MEHP inhibited tryptophan uptake from the medium, then excess of tryptophan should rescue the MEHP-sensitivity of *trp* mutants. To test this possibility, we compared the MEHP-sensitivities of the wild type and 5 *trp* mutants in the presence and absence of 4 mM tryptophan. Addition of tryptophan rescued the sensitivity of all the 5 *trp* mutants (Fig. 3B). Our results are consistent with the hypothesis that MEHP affects the uptake of tryptophan from the medium. However, tryptophan did not increase resistance of the wild type strain to MEHP (Fig. 3B) indicating that MEHP inhibits additional processes apart from tryptophan uptake.

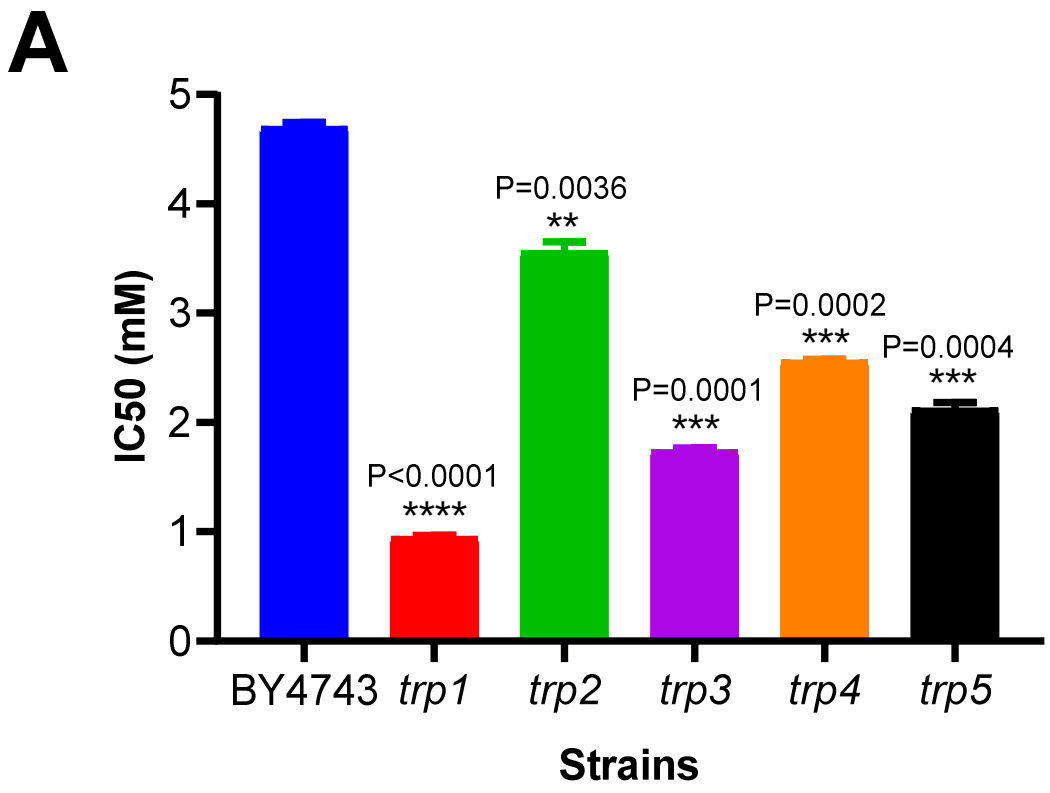
A
IC50 (mM)
5
4
3
2
1
0
P=0.0036
**
P=0.0002
***
P=0.0004
***
P=0.0001
***
P<0.0001
****
BY4743
trp1
trp2
trp3
trp4
trp5
Strains

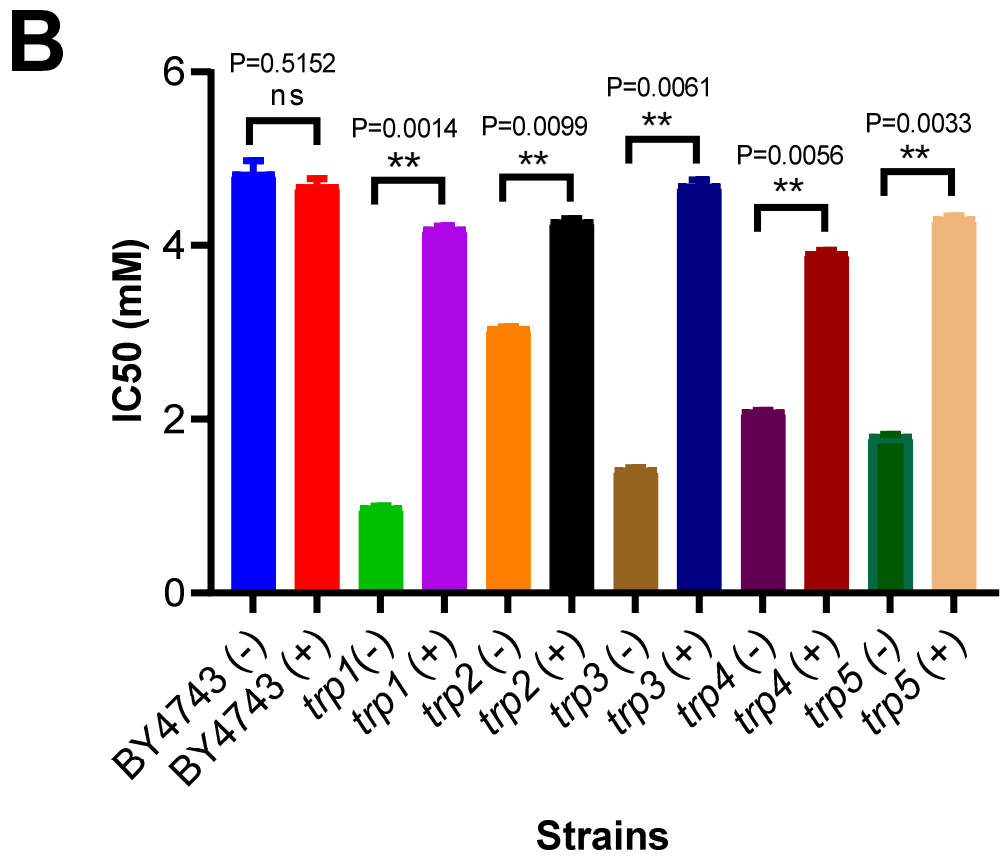
B
IC50 (mM)
6
4
2
0
P=0.5152
ns
P=0.0014
**
P=0.0099
**
P=0.0061
**
P=0.0056
**
P=0.0033
**
BY4743 (-)
BY4743 (+)
trp1(-)
trp1 (+)
trp2 (-)
trp2 (+)
trp3 (-)
trp3 (+)
trp4 (-)
trp4 (+)
trp5 (-)
trp5 (+)
Strains

355

Fig. 3. Tryptophan biosynthetic genes provide resistance to MEHP-toxicity.

A. Wild type strain (BY4743) and tryptophan biosynthetic mutants (*trp1*, *trp2*, *trp3*, *trp4* and *trp5*) were grown in YPD-HEPES (YPD + 25 mM HEPES, pH=6.8) at 30°C in the presence of indicated concentrations of MEHP. IC50 of each strain was calculated after 24 hours of incubation with MEHP. Statistical significance was determined using the unpaired Student's t-test ($P<0.05$).

B. MEHP-toxicity rescue experiment performed in the absence (-) and presence (+) of tryptophan (4 mM). Growth of cells grown in YPD-HEPES (YPD + 25 mM HEPES, pH=6.8) at 30°C with indicated concentrations of MEHP was analyzed in the similar way as described above in Fig.3A. IC50 of each strain was calculated after 24 hours of incubation with MEHP. Statistical significance was determined using the paired Student's t-test ($P<0.05$). ns = not statistically significant ($P>0.05$).

3.4. Mutations in ergosterol biosynthesis are sensitive to MEHP

MEHP showed a genetic interaction with ergosterol biosynthetic gene deletions. Deletion of *ELO2* that encodes an enzyme involved in sphingolipid biosynthesis conferred sensitivity to MEHP (Fig. 1C). Ergosterol and sphingolipids are important constituents of yeast plasma membrane (Simons and Sampaio, 2011; Sharma et al., 2014; Bari et al., 2015). Both lipids form distinct domains called as lipid rafts on the plasma membrane (Simons and Ikonen, 1997; Simons and Sampaio, 2011; Sharma et al., 2014). These dynamic domains are associated with numerous biological functions including endocytosis, protein trafficking and vacuolar biogenesis (Simons and Ikonen, 1997; Simons and Sampaio, 2011; Anderson et al., 2014; Sharma et al., 2014). These biological functions can be compromised by sequestration of ergosterol in the plasma membrane by the polyene antifungal amphotericin B (Anderson et al.,

2014). We explored the MEHP-interaction with mutations that affect ergosterol biosynthesis. We tested MEHP-toxicity for final steps of ergosterol biosynthetic genes (*ERG6, ERG2, ERG3, ERG5* and *ERG4*) (Dupont et al., 2012). Strains lacking *ERG2* and *ERG3* were not present in our HOP assay but we included them in our experiment for comparison with other *erg* mutants. All the 5 *erg* mutants were sensitive to MEHP as compared to wild type strain (Fig. 4A) but not to DEHP (Supplementary Fig. S1C). Among the 5 mutants, ***erg6Δ*** was most sensitive (8-fold) in comparison to wild type strain. The *erg2* mutant was 2.5-fold, *erg3* and *erg5* mutants were 1.6-fold and *erg4* mutant was 3-fold sensitive to MEHP in comparison to the wild type strain (Fig. 4A).

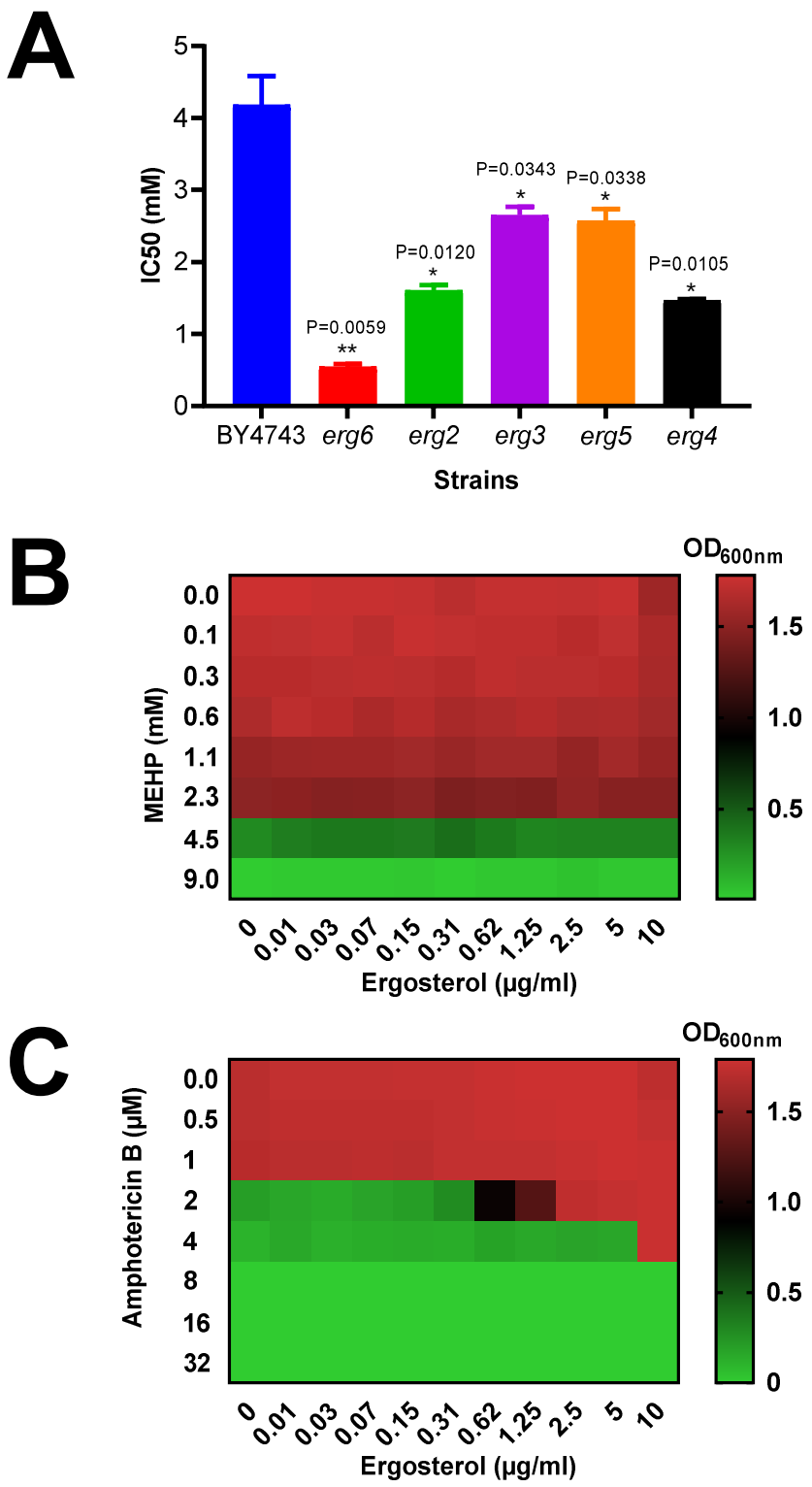

393

394

395

396

Fig. 4. Ergosterol biosynthetic genes provide resistance to MEHP-toxicity.

A. Wild type strain (BY4743) and ergosterol biosynthetic mutants (*erg6*, *erg2*, *erg3*, *erg5* and *erg4*) were grown in YPD-HEPES (YPD + 25 mM HEPES, pH=6.8) at 30°C in the presence of indicated concentrations of MEHP. IC50 of each strain was calculated after 24 hours of incubation with MEHP. Statistical significance was determined using the paired Student's t-test ($P<0.05$).

B. MEHP-toxicity rescue experiment for wild type strain (BY4743) was performed in the presence of ergosterol at indicated concentrations. Growth of cells grown in YPD-HEPES (YPD + 25 mM HEPES, pH=6.8) at 30°C with indicated concentrations of MEHP was analyzed. Growth heat map is shown in the figure. Two independent experiments were performed.

C. Amphotericin B-toxicity rescue experiment for wild type strain (BY4743) was performed and analyzed in the similar way as described above in Fig.4B.

3.5. Toxicity of MEHP is not *via* interaction with ergosterol

To determine whether MEHP affects yeast cells by binding to ergosterol, we tested whether pre-incubation of MEHP with ergosterol reduces its toxicity. MEHP was pre-incubated with ergosterol for an hour before addition to the cells. We used amphotericin B as a positive control that is known to interact with ergosterol (Anderson et al., 2014). Pre-incubation with ergosterol did not affect the toxicity of MEHP (Fig. 4B). However, ergosterol partially rescued the toxicity of amphotericin B (Fig. 4C). These results indicate that MEHP-induced toxic effect is not due to inhibition of ergosterol biosynthesis.

3.6. Mutants defective in cellular transport are sensitive to MEHP

MEHP displayed a genetic interaction with mutations affecting cellular transport. Most of the genes of this class are directly or indirectly involved in membrane trafficking and related functions such as endocytosis, intracellular protein transport, vesicular trafficking and vacuolar protein transport (Supplementary table. 1). Moreover, the terms 'plasma membrane part', 'plasma membrane' and 'internal side of plasma membrane' are enriched among 'Cellular component' and 'phosphoinositide binding', 'phospholipid binding' and 'lipid binding' are enriched among the GO 'Molecular function' categories (Supplementary table. 1). We validated the HOP results for few mutants of these categories and found them to be sensitive to MEHP (Fig. 5) but not to DEHP (Supplementary Fig. S1D). These results suggest that defects in membrane-associated biological processes confer sensitivity to MEHP.

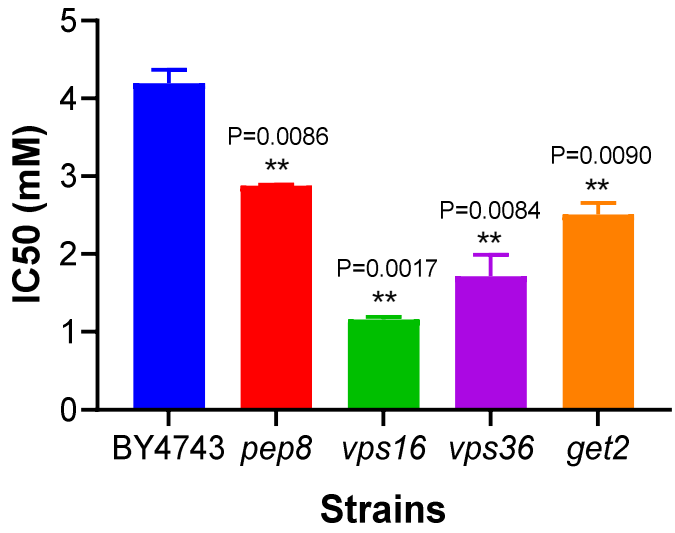

Fig. 5. Cellular transport genes provide resistance to MEHP-toxicity.

Wild type strain (BY4743) and cellular transport mutants (*pep8*, *vps16*, *vps36* and *get2*) were grown in YPD-HEPES (YPD + 25 mM HEPES, pH=6.8) at 30°C in the

presence of indicated concentrations of MEHP. Growth was measured after 24 hours of incubation for each strain. IC50 of each strain was calculated after 24 hours of incubation with MEHP. Statistical significance was determined using the paired Student's t-test ($P<0.05$).

3.7. MEHP induces ionic stress

Alteration in sterol composition of plasma membranes is associated with ionic stress (Kodedova and Sychrova, 2015). Ergosterol biosynthetic mutants (*erg6, erg2, erg3, erg5* and *erg4*) exhibit hyperpolarized plasma membranes and are sensitive to ionic stress (Kodedova and Sychrova, 2015). Plasma membrane hyperpolarization has been reported to be a major contributing factor of cytotoxic cations tolerance such as Na^+ and hygromycin B (Navarre and Goffeau, 2000; Maresova et al., 2009). Cellular transport mutants are also defective in cytotoxic cation tolerance (Fell et al., 2011). We tested whether MEHP causes ionic stress to yeast cells. We tested the effect of MEHP on sensitivity of yeast cells to NaCl and the positively charged drug hygromycin B. We included the non-ionic compound sorbitol as a control. We found that MEHP works synergistically with NaCl and hygromycin B (Fig. 6A-B; Supplementary table. S2). In contrast, addition of sorbitol did not affect the MEHP-sensitivity of yeast cells (Fig. 6A-B; Supplementary table. S2). DEHP did not affect the sensitivities of yeast cells to NaCl, hygromycin and sorbitol (Supplementary Fig. S2; Supplementary table. S2). Together, our data suggests that MEHP induces ionic but not osmotic stress in yeast cells.

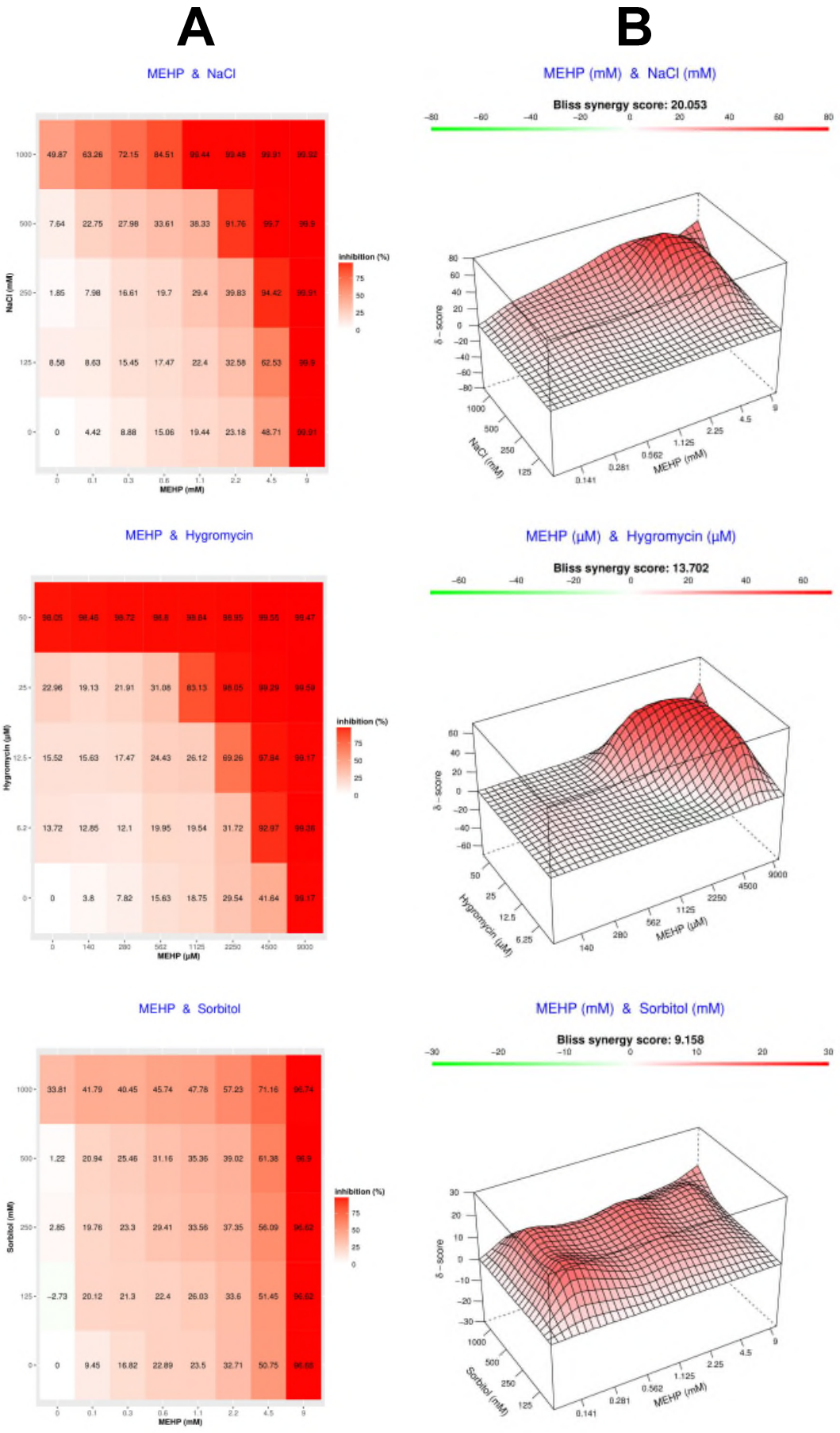
A
B
MEHP & NaCl
MEHP (mM) & NaCl (mM)
Bliss synergy score: 20.053
MEHP & Hygromycin
MEHP (μM) & Hygromycin (μM)
Bliss synergy score: 13.702
MEHP & Sorbitol
MEHP (mM) & Sorbitol (mM)
Bliss synergy score: 9.158
inhibition (%)
δ – score
NaCl (mM)
Hygromycin (μM)
Sorbitol (mM)
MEHP (mM)
MEHP (μM)

464

Fig. 6. MEHP induce ionic stress in yeast cells.

A. Wild type strain (BY4743) was grown in YPD-HEPES (YPD + 25 mM HEPES, pH=6.8) at 30°C in the presence of indicated concentrations of MEHP and NaCl or hygromycin or sorbitol. Growth at the different concentrations was recorded after 24 hours. Dose−response matrix (% growth inhibition) (Fig. 6A) and their corresponding Bliss synergy scores visualized by 3D synergy map (Fig. 6B). Two independent experiments were performed.

3.8. MEHP interacts with plasma membrane and protects yeast cells from membrane perturbing agents

Several cationic amphipathic drugs cause ionic instability by preferentially interacting with plasma membrane (Maresova et al., 2009). Moreover, Molecular Function enrichment analysis indicated that several of the MEHP-resistance gene products bound to membrane lipids. We therefore tested whether MEHP inhibits yeast cells by interacting with the plasma membrane. To explore this possibility, we investigated whether there was any interaction of MEHP with the sterol-binding agent amphotericin B (AmB) and two sphingolipid biosynthetic intermediates dihydrosphingosine (DHS) and phytosphingosine (PHS). AmB, DHS and PHS exert cytotoxic effect by binding to membrane and causing cell lysis (Veerman et al., 2010; Anderson et al., 2014). We performed a combinatorial growth assay with different concentrations of MEHP and AmB or MEHP and DHS or MEHP and PHS. We found that poor growth of AmB- or DHS- or PHS- treated cells was partially rescued by MEHP (Fig. 7A-B; Supplementary table. S3). Notably, the antagonistic interaction phenotype was observed at sublethal concentrations of MEHP, nonetheless toxicity was observed at higher concentrations

of MEHP (Fig. 7A-B; Supplementary table. S3). In contrast to MEHP, DEHP failed to rescue the cytotoxicity of AmB, DHS and PHS (Supplementary Fig. S3; Supplementary table. S3). Our results are consistent with the hypothesis that MEHP protects yeast cells from AmB, PHS and DHS by competing with them for binding sites on the plasma membrane.

A

B

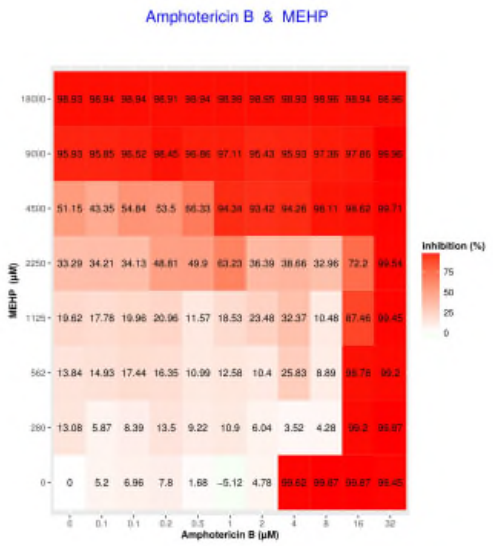
Amphotericin B & MEHP
MEHP (μM)
Amphotericin B (μM)
Inhibition (%)

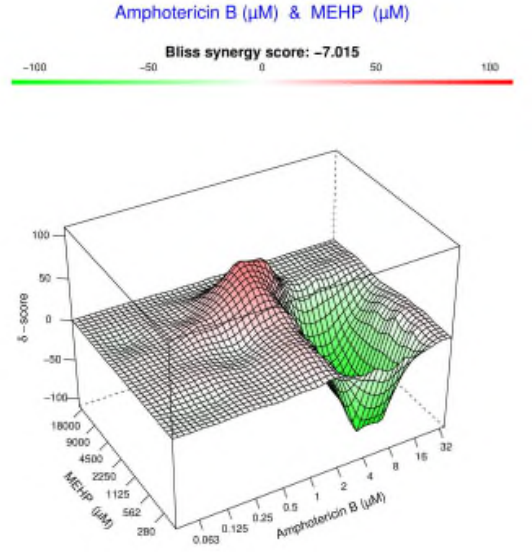
Amphotericin B (μM) & MEHP (μM)
Bliss synergy score: −7.015
δ−score
MEHP (μM)
Amphotericin B (μM)

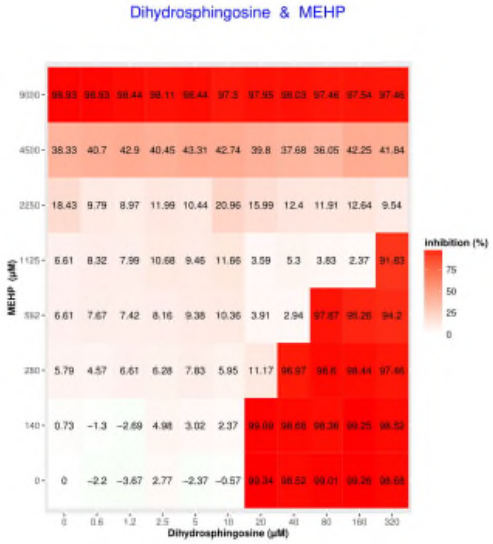
Dihydrosphingosine & MEHP
MEHP (μM)
Dihydrosphingosine (μM)
Inhibition (%)

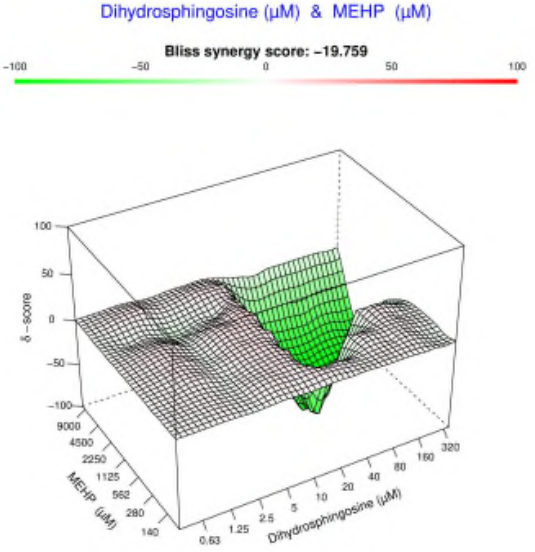
Dihydrosphingosine (μM) & MEHP (μM)
Bliss synergy score: −19.759
δ−score
MEHP (μM)
Dihydrosphingosine (μM)

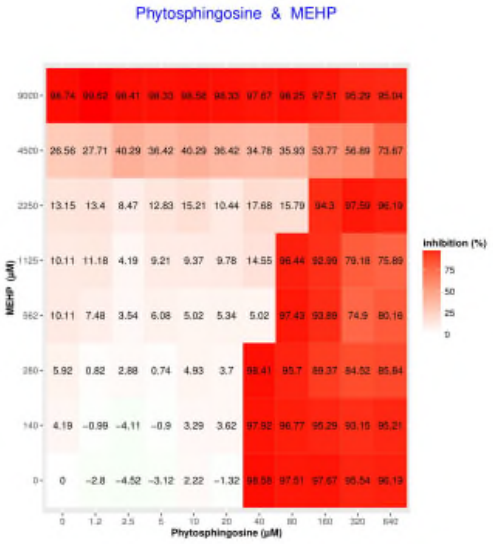
Phytosphingosine & MEHP
MEHP (μM)
Phytosphingosine (μM)
Inhibition (%)

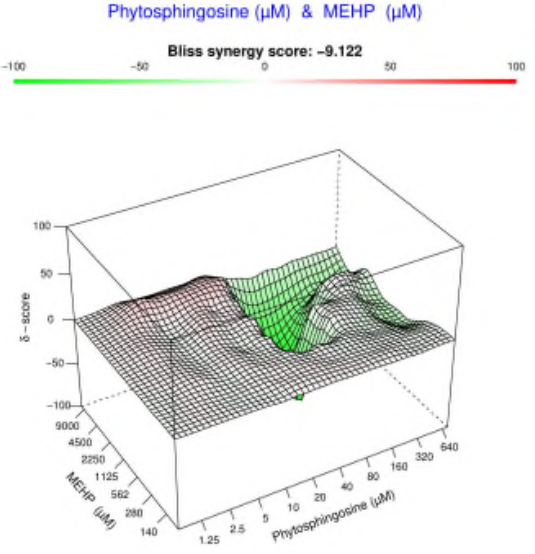
Phytosphingosine (μM) & MEHP (μM)
Bliss synergy score: −9.122
δ−score
MEHP (μM)
Phytosphingosine (μM)

497

Fig. 7. MEHP antagonistically interacts with membrane-perturbing agent amphotericin B, dihydrosphingosine and phytosphingosine

Wild type strain (BY4743) were grown in YPD-HEPES (YPD + 25 mM HEPES, pH=6.8) at 30°C in the presence of indicated concentrations of MEHP and amphotericin B or dihydrosphingosine or phytosphingosine. Growth at the different concentrations was recorded after 24 hours. Dose-response matrix (% growth inhibition) (Fig. 7A) and their corresponding Bliss synergy scores visualized by 3D synergy map (Fig. 7B). Two independent experiments were performed.

3.9. MEHP disrupts the integrity of plasma membrane and cell wall

To determine whether MEHP affects the integrity of yeast plasma membranes, we tested the effect of MEHP on the uptake of the membrane impermeant dye propidium iodide (PI). Yeast cells were treated with either MEHP or DEHP or DMSO for 4 hours. After that cells were incubated with PI and visualized by fluorescence microscopy. 98% of DMSO-treated cells (control) failed to take up PI as expected (Fig. 8A-B). About 96% of cells treated with MEHP (9 mM) had internalized PI (Fig. 8A-B). Internalization of PI caused by MEHP was dose-dependent. In contrast, less than 3% of the DEHP–treated cells had PI staining (Fig. 8A-B). These results indicate that MEHP disrupts the membrane integrity of yeast cells.

As plasma membrane together with cell wall provides protection to the yeast cell from environment, we examined the effect of MEHP on cell wall integrity by calcofluor white (CFW) staining. CFW has been extensively used to visualise and examined the integrity of the yeast cell wall (Alfatah et al., 2017). We classified the cells into two categories based on CFW staining. Cells with peripheral CFW staining were classified

523 as ‘normal cell wall’ and those with cytoplasmic staining were classified as ‘defective
524 cell wall’ (Fig. 9A). About 98% of 9 mM MEHP-treated cells had defective cell walls
525 (Fig. 9B). However, only 2% of DMSO-treated (control) cells had defective cell walls.
526 DEHP treatment had no effect on cell wall integrity (Fig. 9B). Our results revealed that
527 MEHP damages the integrity of plasma membrane and cell wall of yeast cells.

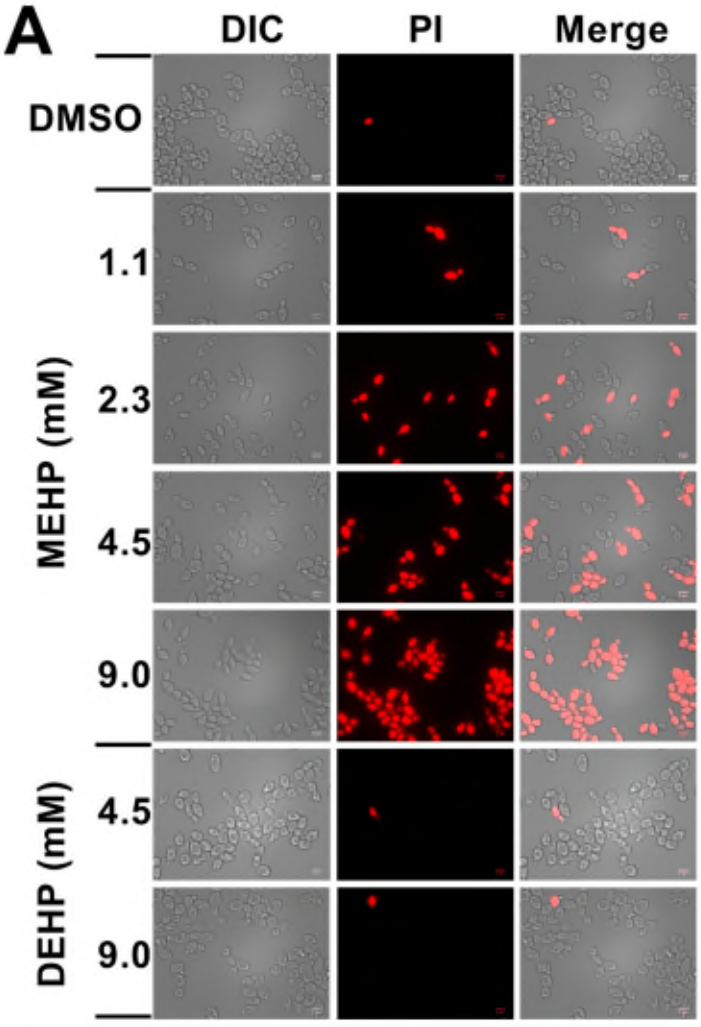

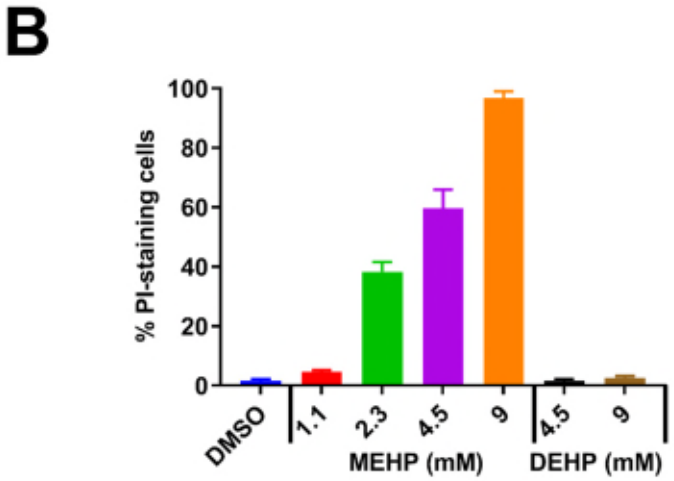

528

529

530

531

Fig. 8. MEHP disrupts the plasma membrane integrity of yeast cells.

A. Wild type yeast cells pre-treated with either DMSO or MEHP or DEHP at indicated concentrations for 4 hours. They were then incubated with propidium iodide (PI) and analyzed by bright field and fluorescence microscopy. Scale bar = 5 μm.

B. Representative images of cells are shown along with quantification of PI-staining cells (N≥100 cells). Representative data from two independent experiments are shown in the figure.

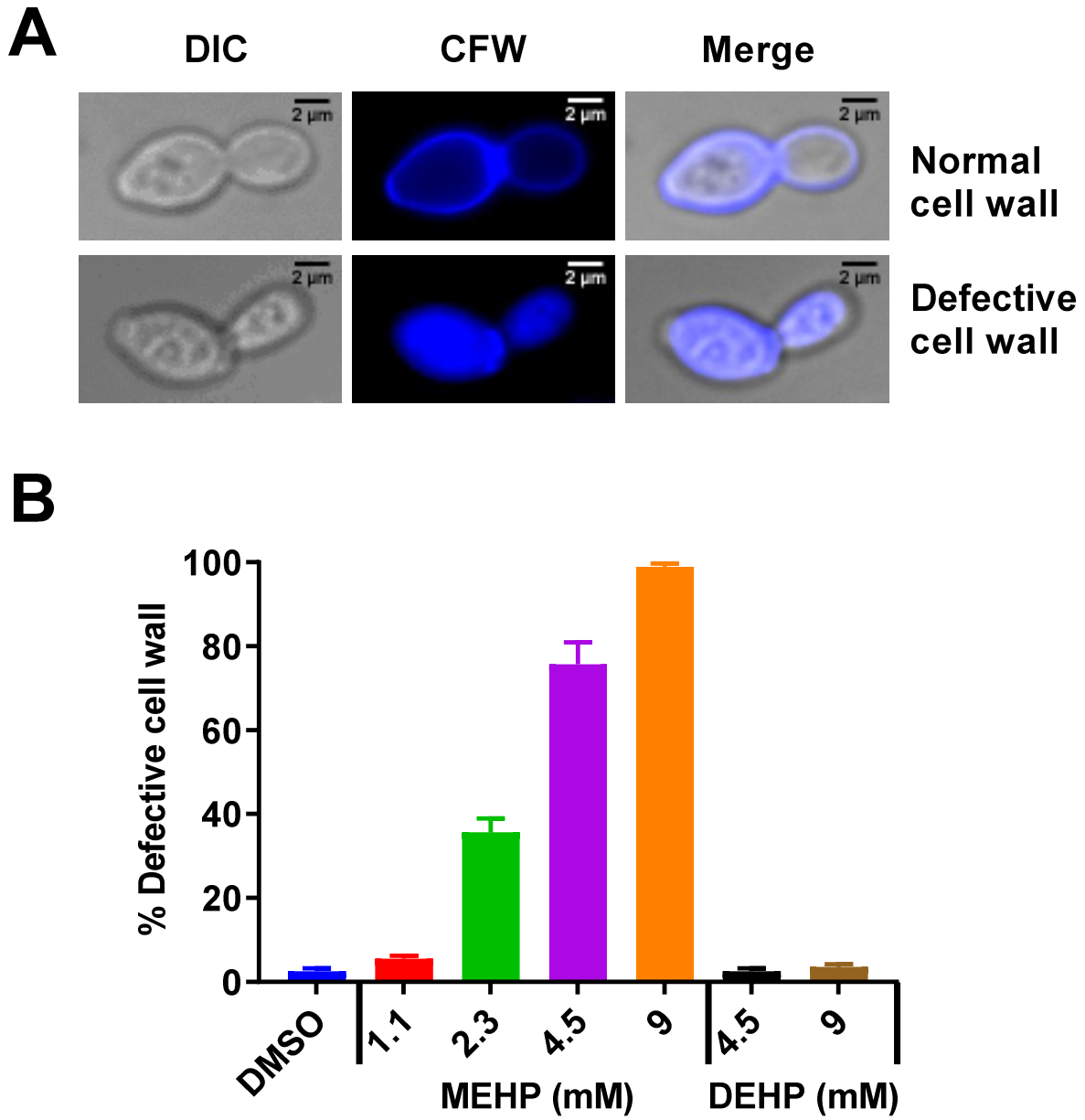

Fig. 9. MEHP disrupts the cell wall integrity of yeast cells.

A. Wild type yeast cells pre-treated with either DMSO or MEHP or DEHP at indicated concentrations for 4 hours. They were then incubated with calcofluor white (CFW) and analyzed by bright field and fluorescence microscopy. Scale bar = 2 µm.

B. Representative images of cells are shown along with quantification of CFW-staining cells (N≥100 cells). Representative data from two independent experiments are shown in the figure.

4. Discussion

MEHP has been linked to a plethora of human diseases, including cancer, diabetes, obesity and lung inflammation (Kamrin, 2009; Braun et al., 2013; Benjamin et al., 2017; Rafael-Vazquez et al., 2018). It has also been implicated in causing hepatotoxicity and reproductive toxicity (Rowdhwal and Chen, 2018). But how this bioactive metabolite of DEHP modulates biological functions and causes its adverse cellular effects is poorly understood. Previous studies showed that MEHP induces oxidative stress, lipid peroxidation, DNA damage and inhibits steroid production (Wang et al., 2012; Yang et al., 2012; Tetz et al., 2013; Craig et al., 2014; Sobarzo et al., 2015). We found that MEHP but not DEHP was toxic to yeast cells which mirrored their relative effects in mammalian system. We therefore undertook a comprehensive elucidation of genetic interactions in yeast to unravel the spectrum of biological functions affected by MEHP. Gene Ontology enrichment analysis of the 218 genes that when deleted confer sensitivity to MEHP identified seven functional categories affected by MEHP. They are (1) cellular amino acid biosynthetic process, (2) sterol biosynthetic process, (3) cellular transport, (4) transcriptional and translational regulation, (5) protein glycosylation, (6) cytokinesis and cell morphogenesis and (7) ionic homeostasis.

Tryptophan biosynthetic genes (*TRP1, TRP2, TRP3, TRP4* and *TRP5)* were most dominant in the first functional category. Deletion strains lacking these genes displayed enhanced sensitivity to MEHP as compared to wild type strain. Similar results were reported in a recent genome-wide study of MEHP sensitivity in yeast (Jiang et al., 2018). Sensitivity of the *trp* mutants was rescued by addition of tryptophan. As the *trp* auxotrophic mutants require uptake of tryptophan from the medium, it is conceivable that MEHP binds to the plasma membrane and inhibits the activity of tryptophan transporters. Interestingly, tryptophan provides protection to

yeast cells from various forms of stress such as plasma membrane damage (Ikui et al., 2018) and DNA damage (Godin et al., 2016). Additionally, tryptophan delays free radical generation by modulating activity of superoxide dismutase activity and provides resistance to oxidative stress and lipid peroxidation in heterophils of ringdove (Paredes et al., 2009). As MEHP causes oxidative and DNA damage stress in mammalian cells (Inada et al., 2012; Wang et al., 2012; Yang et al., 2012; Tetz et al., 2013; Sobarzo et al., 2015), the *trp* mutants having presumably lower tryptophan levels than wild type strain could be more sensitive to MEHP.

Multiple mutants defective in ergosterol biosynthesis (*erg6, erg2, erg3, erg5* and *erg4*) were sensitive to MEHP. Deletion of the sphingolipid biosynthetic gene *ELO2* fatty acid elongase, which is involved in the synthesis of very long chain C24 fatty acids (Alfatah et al., 2017) also conferred sensitivity to MEHP. Sterols (ergosterol in fungi and cholesterol in higher eukaryotes) interact physically and functionally with sphingolipids (Guan et al., 2009; Breslow and Weissman, 2010) forming distinct domains in plasma membrane called lipid rafts. An intriguing possibility is that MEHP could bind to lipid rafts in yeast and thereby affect plasma membrane function. Consistent with this hypothesis, MEHP partially rescued the toxicity of sterol-binding drug amphotericin B and sphingolipid intermediates namely dihydrosphingosine and phytoshingosine. The hypothesis would also explain why mutants defective in vacuolar transport are sensitive to MEHP as lipid rafts are required for several cellular processes including endocytosis, protein sorting and maintenance of plasma membrane integrity (Simons and Ikonen, 1997; Simons and Sampaio, 2011). Interestingly, a functional association of MEHP with sterols has been reported in mammalian cells (Craig et al., 2014; Rowdhwal and Chen, 2018). MEHP mediated deregulation of sterol/lipid synthesis has been reported to cause hepatotoxicity and

reproductive toxicity (Muczynski et al., 2012; Zhou et al., 2013; Zhang et al., 2017; Rowdhwal and Chen, 2018). MEHP interaction with lipid also shown in the previous study in yeast (Jiang et al., 2018). Thus, MEHP-interaction with lipids appears to be conserved between yeast and human cells.

In contrast to MEHP, DEHP did not have any inhibitory effect on yeast cells in the various assays tested. Presence of the free carboxyl group appears to be essential for MEHP's toxicity in both yeast and mammalian cells. The carboxyl group in MEHP might make it more amphipathic in comparison to DEHP and aid its insertion into the plasma membrane. It would be informative to compare the interaction of MEHP and DEHP with artificial membranes like liposomes.

In summary, our findings provide new insights into the mode-of-action of MEHP on cellular systems. We show that MEHP compromises the integrity of the yeast plasma membrane and cell wall. This provides a basis for why several yeast mutants defective in membrane-related functions are sensitive to MEHP. It will be interesting to test whether our observations on MEHP toxicity are extendable to mammalian cells.

Acknowledgements

We are grateful to the funding provided by the Bioinformatics Institute (BII), Biomedical Research Council (BMRC)—Economic Development Board (EDB) Industry Alignment Fund (IAF311017G) and Agency for Science, Technology and Research (A*STAR), Singapore. We thank Dr Lit-Hsin Loo for providing us DEHP and Dr Melvin Anderson for suggesting us to investigate the mode-of-action of MEHP by chemogenomic profiling.

Author Contributions Statement

PA and MA conceived and supervised the experiments. MA and JH performed the HOP assay and analyzed the HOP data. SH supervised the NGS analysis of barcode sequences performed by KWK and analyzed the HOP data. MA and FU performed the experiments. MA, JH, FU and PA analyzed the results. PA and MA wrote the paper and all authors reviewed the paper.

Competing interests

The authors declare no competing financial and non-financial interests.

References

Albro, P.W., Thomas, R.O., 1973. Enzymatic hydrolysis of Di-(2-ethylhexyl) phthalate by lipases. Biochimica et Biophysica Acta (BBA) - Lipids and Lipid Metabolism 306, 380-390.

Alfatah, M., Bari, V.K., Nahar, A.S., Bijlani, S., Ganesan, K., 2017. Critical role for CaFEN1 and CaFEN12 of Candida albicans in cell wall integrity and biofilm formation. Sci Rep 7, 40281.

Alfatah, M., Wong, J.H., Nge, C.E., Kong, K.W., Low, K.N., Leong, C.Y., Crasta, S., Munusamy, M., Chang, A.M.L., Hoon, S., 2019. Hypoculoside, a sphingoid base-like compound from Acremonium disrupts the membrane integrity of yeast cells. Scientific reports 9, 710.

Anderson, T.M., Clay, M.C., Cioffi, A.G., Diaz, K.A., Hisao, G.S., Tuttle, M.D., Nieuwkoop, A.J., Comellas, G., Maryum, N., Wang, S., Uno, B.E., Wildeman, E.L., Gonen, T., Rienstra, C.M., Burke, M.D., 2014. Amphotericin forms an extramembranous and fungicidal sterol sponge. Nat Chem Biol 10, 400-406.

Bari, V.K., Sharma, S., Alfatah, M., Mondal, A.K., Ganesan, K., 2015. Plasma Membrane Proteolipid 3 Protein Modulates Amphotericin B Resistance through Sphingolipid Biosynthetic Pathway. Sci Rep 5, 9685.

Benjamin, S., Masai, E., Kamimura, N., Takahashi, K., Anderson, R.C., Faisal, P.A., 2017. Phthalates impact human health: Epidemiological evidences and plausible mechanism of action. J Hazard Mater 340, 360-383.

Bonilla, E., del Mazo, J., 2010. Deregulation of the Sod1 and Nd1 genes in mouse fetal oocytes exposed to mono-(2-ethylhexyl) phthalate (MEHP). Reprod Toxicol 30, 387-392.

Braun, J.M., Sathyanarayana, S., Hauser, R., 2013. Phthalate exposure and children's health. Curr Opin Pediatr 25, 247-254.

Breslow, D.K., Weissman, J.S., 2010. Membranes in balance: mechanisms of sphingolipid homeostasis. Mol Cell 40, 267-279.

Cao, X.-L., 2010. Phthalate Esters in Foods: Sources, Occurrence, and Analytical Methods. Comprehensive Reviews in Food Science and Food Safety 9, 21-43.

Carpenter, D.O., Arcaro, K., Spink, D.C., 2002. Understanding the human health effects of chemical mixtures. Environ Health Perspect 110 Suppl 1, 25-42.

Craig, Z.R., Singh, J., Gupta, R.K., Flaws, J.A., 2014. Co-treatment of mouse antral follicles with 17beta-estradiol interferes with mono-2-ethylhexyl phthalate (MEHP)-induced atresia and altered apoptosis gene expression. Reprod Toxicol 45, 45-51.

Dupont, S., Lemetais, G., Ferreira, T., Cayot, P., Gervais, P., Beney, L., 2012. ERGOSTEROL BIOSYNTHESIS: A FUNGAL PATHWAY FOR LIFE ON LAND? Evolution 66, 2961-2968.

Fell, G.L., Munson, A.M., Croston, M.A., Rosenwald, A.G., 2011. Identification of yeast genes involved in k homeostasis: loss of membrane traffic genes affects k uptake. G3 (Bethesda) 1, 43-56.

Gao, D.W., Wen, Z.D., 2016. Phthalate esters in the environment: A critical review of their occurrence, biodegradation, and removal during wastewater treatment processes. Sci Total Environ 541, 986-1001.

Giaever, G., Flaherty, P., Kumm, J., Proctor, M., Nislow, C., Jaramillo, D.F., Chu, A.M., Jordan, M.I., Arkin, A.P., Davis, R.W., 2004. Chemogenomic profiling: identifying the functional interactions of small molecules in yeast. Proc Natl Acad Sci U S A 101, 793-798.

Godin, S.K., Lee, A.G., Baird, J.M., Herken, B.W., Bernstein, K.A., 2016. Tryptophan biosynthesis is important for resistance to replicative stress in *Saccharomyces cerevisiae*. Yeast 33, 183-189.

Guan, X.L., Souza, C.M., Pichler, H., Dewhurst, G., Schaad, O., Kajiwara, K., Wakabayashi, H., Ivanova, T., Castillon, G.A., Piccolis, M., Abe, F., Loewith, R., Funato, K., Wenk, M.R., Riezman, H., 2009. Functional interactions between sphingolipids and sterols in biological membranes regulating cell physiology. Mol Biol Cell 20, 2083-2095.

Halden, R.U., 2010. Plastics and health risks. Annu Rev Public Health 31, 179-194.

Haque, F., Alfatah, M., Ganesan, K., Bhattacharyya, M.S., 2016. Inhibitory Effect of Sophorolipid on Candida albicans Biofilm Formation and Hyphal Growth. Sci Rep 6, 23575.

693 Heudorf, U., Mersch-Sundermann, V., Angerer, J., 2007. Phthalates: Toxicology and exposure.
694 International Journal of Hygiene and Environmental Health 210, 623-634.
695 Hillenmeyer, M.E., Ericson, E., Davis, R.W., Nislow, C., Koller, D., Giaever, G., 2010. Systematic
696 analysis of genome-wide fitness data in yeast reveals novel gene function and drug action. Genome
697 Biol 11, R30.
698 Hoon, S., Smith, A.M., Wallace, I.M., Suresh, S., Miranda, M., Fung, E., Proctor, M., Shokat, K.M.,
699 Zhang, C., Davis, R.W., Giaever, G., St Onge, R.P., Nislow, C., 2008. An integrated platform of genomic
700 assays reveals small-molecule bioactivities. Nat Chem Biol 4, 498-506.
701 Huang da, W., Sherman, B.T., Lempicki, R.A., 2009a. Bioinformatics enrichment tools: paths toward
702 the comprehensive functional analysis of large gene lists. Nucleic Acids Res 37, 1-13.
703 Huang da, W., Sherman, B.T., Lempicki, R.A., 2009b. Systematic and integrative analysis of large gene
704 lists using DAVID bioinformatics resources. Nat Protoc 4, 44-57.
705 Ianevski, A., He, L., Aittokallio, T., Tang, J., 2017. SynergyFinder: a web application for analyzing drug
706 combination dose–response matrix data. Bioinformatics 33, 2413-2415.
707 Ikui, A., Schroeder, L., Lazarevskiy, P., 2018. Tryptophan recovers sensitivity to cell membrane stress
708 in *Saccharomyces cerevisiae*. bioRxiv.
709 Inada, H., Chihara, K., Yamashita, A., Miyawaki, I., Fukuda, C., Tateishi, Y., Kunimatsu, T., Kimura, J.,
710 Funabashi, H., Miyano, T., 2012. Evaluation of ovarian toxicity of mono-(2-ethylhexyl) phthalate
711 (MEHP) using cultured rat ovarian follicles. J Toxicol Sci 37, 483-490.
712 Jaishankar, M., Tseten, T., Anbalagan, N., Mathew, B.B., Beeregowda, K.N., 2014. Toxicity,
713 mechanism and health effects of some heavy metals. Interdiscip Toxicol 7, 60-72.
714 Jiang, L., Wang, L., Fang, T., Papadopoulos, V., 2018. Disruption of ergosterol and tryptophan
715 biosynthesis, as well as cell wall integrity pathway and the intracellular pH homeostasis, lead to
716 mono-(2-ethylhexyl)-phthalate toxicity in budding yeast. Chemosphere 206, 643-654.
717 Kamrin, M.A., 2009. Phthalate risks, phthalate regulation, and public health: a review. J Toxicol
718 Environ Health B Crit Rev 12, 157-174.
719 Kodedova, M., Sychrova, H., 2015. Changes in the Sterol Composition of the Plasma Membrane
720 Affect Membrane Potential, Salt Tolerance and the Activity of Multidrug Resistance Pumps in
721 Saccharomyces cerevisiae. PLoS One 10, e0139306.
722 Kola, I., Landis, J., 2004. Can the pharmaceutical industry reduce attrition rates? Nat Rev Drug Discov
723 3, 711-715.
724 Kramer, J.A., Sagartz, J.E., Morris, D.L., 2007. The application of discovery toxicology and pathology
725 towards the design of safer pharmaceutical lead candidates. Nat Rev Drug Discov 6, 636-649.
726 Kratochvil, I., Hofmann, T., Rother, S., Schlichting, R., Moretti, R., Scharnweber, D., Hintze, V., Escher,
727 B.I., Meiler, J., Kalkhof, S., Bergen, M., MEHP and MEOHP but not DEHP bind productively to the
728 peroxisome proliferator-activated receptor γ. Rapid Communications in Mass Spectrometry 0.
729 Lioy, P.J., Hauser, R., Gennings, C., Koch, H.M., Mirkes, P.E., Schwetz, B.A., Kortenkamp, A., 2015.
730 Assessment of phthalates/phthalate alternatives in children's toys and childcare articles: Review of
731 the report including conclusions and recommendation of the Chronic Hazard Advisory Panel of the
732 Consumer Product Safety Commission. J Expo Sci Environ Epidemiol 25, 343-353.
733 Maresova, L., Muend, S., Zhang, Y.Q., Sychrova, H., Rao, R., 2009. Membrane hyperpolarization
734 drives cation influx and fungicidal activity of amiodarone. J Biol Chem 284, 2795-2802.
735 Muczynski, V., Lecureuil, C., Messiaen, S., Guerquin, M.-J., N'Tumba-Byn, T., Moison, D., Hodroj, W.,
736 Benjelloun, H., Baijer, J., Livera, G., 2012. Cellular and molecular effect of MEHP involving LXRα in
737 human fetal testis and ovary. PloS one 7, e48266.
738 Navarre, C., Goffeau, A., 2000. Membrane hyperpolarization and salt sensitivity induced by deletion
739 of PMP3, a highly conserved small protein of yeast plasma membrane. EMBO J 19, 2515-2524.
740 Ng, S.M.S., Yap, J.M., Lau, Q.Y., Ng, F.M., Ong, E.H.Q., Barkham, T., Teo, J.W.P., Alfatah, M., Kong,
741 K.W., Hoon, S., Arumugam, P., Hill, J., Brian Chia, C.S., 2018. Structure-activity relationship studies of
742 ultra-short peptides with potent activities against fluconazole-resistant Candida albicans. Eur J Med
743 Chem 150, 479-490.

744 Paredes, S.D., Bejarano, I., Terron, M.P., Barriga, C., Reiter, R.J., Rodriguez, A.B., 2009. Melatonin and
745 tryptophan counteract lipid peroxidation and modulate superoxide dismutase activity in ringdove
746 heterophils in vivo. Effect of antigen-induced activation and age. Age (Dordr) 31, 179-188.
747 Rafael-Vazquez, L., Garcia-Trejo, S., Aztatzi-Aguilar, O.G., Bazan-Perkins, B., Quintanilla-Vega, B.,
748 2018. Exposure to diethylhexyl phthalate (DEHP) and monoethylhexyl phthalate (MEHP) promotes
749 the loss of alveolar epithelial phenotype of A549 cells. Toxicol Lett 294, 135-144.
750 Robinson, M.D., McCarthy, D.J., Smyth, G.K., 2010. edgeR: a Bioconductor package for differential
751 expression analysis of digital gene expression data. Bioinformatics 26, 139-140.
752 Rowdhwal, S.S.S., Chen, J., 2018. Toxic Effects of Di-2-ethylhexyl Phthalate: An Overview. BioMed
753 Research International 2018, 10.
754 Rudel, R.A., Perovich, L.J., 2009. Endocrine disrupting chemicals in indoor and outdoor air.
755 Atmospheric Environment 43, 170-181.
756 Saito, T., Hong, P., Tanabe, R., Nagai, K., Kato, K., 2010. Enzymatic hydrolysis of structurally diverse
757 phthalic acid esters by porcine and bovine pancreatic cholesterol esterases. Chemosphere 81, 1544-
758 1548.
759 Serrano, S.E., Braun, J., Trasande, L., Dills, R., Sathyanarayana, S., 2014. Phthalates and diet: a review
760 of the food monitoring and epidemiology data. Environ Health 13, 43.
761 Sharma, S., Alfatah, M., Bari, V.K., Rawal, Y., Paul, S., Ganesan, K., 2014. Sphingolipid biosynthetic
762 pathway genes FEN1 and SUR4 modulate amphotericin B resistance. Antimicrob Agents Chemother
763 58, 2409-2414.
764 Simons, K., Ikonen, E., 1997. Functional rafts in cell membranes. Nature 387, 569-572.
765 Simons, K., Sampaio, J.L., 2011. Membrane organization and lipid rafts. Cold Spring Harb Perspect
766 Biol 3, a004697.
767 Sobarzo, C.M., Rosana Nde, M., Livia, L., Berta, D., Schteingart, H.F., 2015. Mono-(2-ethylhexyl)
768 phthalate (MEHP) affects intercellular junctions of Sertoli cell: A potential role of oxidative stress.
769 Reprod Toxicol 58, 203-212.
770 Stathias, V., Jermakowicz, A.M., Maloof, M.E., Forlin, M., Walters, W., Suter, R.K., Durante, M.A.,
771 Williams, S.L., Harbour, J.W., Volmar, C.H., Lyons, N.J., Wahlestedt, C., Graham, R.M., Ivan, M.E.,
772 Komotar, R.J., Sarkaria, J.N., Subramanian, A., Golub, T.R., Schurer, S.C., Ayad, N.G., 2018. Drug and
773 disease signature integration identifies synergistic combinations in glioblastoma. Nat Commun 9,
774 5315.
775 Stroustrup, A., Bragg, J.B., Busgang, S.A., Andra, S.S., Curtin, P., Spear, E.A., Just, A.C., Arora, M.,
776 Gennings, C., 2018. Sources of clinically significant neonatal intensive care unit phthalate exposure. J
777 Expo Sci Environ Epidemiol.
778 Supek, F., Bosnjak, M., Skunca, N., Smuc, T., 2011. REVIGO summarizes and visualizes long lists of
779 gene ontology terms. PLoS One 6, e21800.
780 Tchounwou, P.B., Yedjou, C.G., Patlolla, A.K., Sutton, D.J., 2012. Heavy metal toxicity and the
781 environment. EXS 101, 133-164.
782 Tetz, L.M., Cheng, A.A., Korte, C.S., Giese, R.W., Wang, P., Harris, C., Meeker, J.D., Loch-Caruso, R.,
783 2013. Mono-2-ethylhexyl phthalate induces oxidative stress responses in human placental cells in
784 vitro. Toxicol Appl Pharmacol 268, 47-54.
785 Veerman, E.C., Valentijn-Benz, M., van't Hof, W., Nazmi, K., van Marle, J., Amerongen, A.V., 2010.
786 Phytosphingosine kills *Candida albicans* by disrupting its cell membrane. Biol Chem 391, 65-71.
787 Wang, W., Craig, Z.R., Basavarajappa, M.S., Hafner, K.S., Flaws, J.A., 2012. Mono-(2-ethylhexyl)
788 phthalate induces oxidative stress and inhibits growth of mouse ovarian antral follicles. Biol Reprod
789 87, 152.
790 Yang, G., Zhou, X., Wang, J., Zhang, W., Zheng, H., Lu, W., Yuan, J., 2012. MEHP-induced oxidative
791 DNA damage and apoptosis in HepG2 cells correlates with p53-mediated mitochondria-dependent
792 signaling pathway. Food Chem Toxicol 50, 2424-2431.
793 Yao, P.L., Lin, Y.C., Richburg, J.H., 2012. Mono-(2-ethylhexyl) phthalate (MEHP) promotes invasion
794 and migration of human testicular embryonal carcinoma cells. Biol Reprod 86, 160, 161-110.

795 Zhang, W., Shen, X.-Y., Zhang, W.-W., Chen, H., Xu, W.-P., Wei, W., 2017. The effects of di 2-ethyl
796 hexyl phthalate (DEHP) on cellular lipid accumulation in HepG2 cells and its potential mechanisms in
797 the molecular level. Toxicology Mechanisms and Methods 27, 245-252.
798 Zhou, L., Beattie, M.C., Lin, C.-Y., Liu, J., Traore, K., Papadopoulos, V., Zirkin, B.R., Chen, H., 2013.
799 Oxidative stress and phthalate-induced down-regulation of steroidogenesis in MA-10 Leydig cells.
800 Reproductive toxicology 42, 95-101.

801

802

Supplementary Material

Chemical-genetic interaction landscape of mono-(2-ethylhexyl)-phthalate using chemogenomic profiling in yeast

Mohammad Alfatah[1]*, Jin Huei Wong[1], Kiat Whye Kong[2], Felix Utama[3], Shawn Hoon[2], and Prakash Arumugam[1]*

1. Bioinformatics Institute, 30 Biopolis Street, #07-01, Matrix, Singapore 138671

2. Molecular Engineering Laboratory, 61 Biopolis Drive, #03-12 Proteos, Singapore 13867

3. School of Chemical and Life Sciences, Singapore Polytechnic, 500 Dover Road, Singapore 139651

*To whom correspondence must be addressed

Email: alfatahm@bii.a-star.edu and prakasha@bii.a-star.edu

Key Words

Mono-(2-ethylhexyl)-phthalate (MEHP); Di-(2-ethylhexyl)-phthalate (DEHP); Chemogenomic profiling; Chemical-genetic interaction; *Saccharomyces cerevisiae*

Primers used in HOP Assay

Reverse primer common (Rc):

5’AATGATACGGCGACCACCGAGATCTACACTCTTTCCCTACACGACGCTCTTCCGATCTGTCCACGAGGTCTCT3’

Forward primer variable (Fv) containing a sample-specific TruSeq index:

5’CAAGCAGAAGACGGCATACGAGATNNNNNNGTGACTGGAGTTCAGACGTGTGCTCTTCCGATCTGTCGACCTGCAGCGTACG3’

Nucleotides indicated in green in Rc and Fv are complementary to sequences flanking the bar-code in the Yeast deletion strains. Nucleotides indicated in red in Rc is the sequence of the Universal Illumina Adaptor. Nucleotides in blue in Fv is the sequence of the Illumina PCR Primer 2.0. Hexanucleotide NNNNNN in Fv is the sample-specific TruSeq index. Nucleotides indicated in orange in Fv is sequence of the Multiplexing Read 2 sequencing primer.

Supplementary Figures:

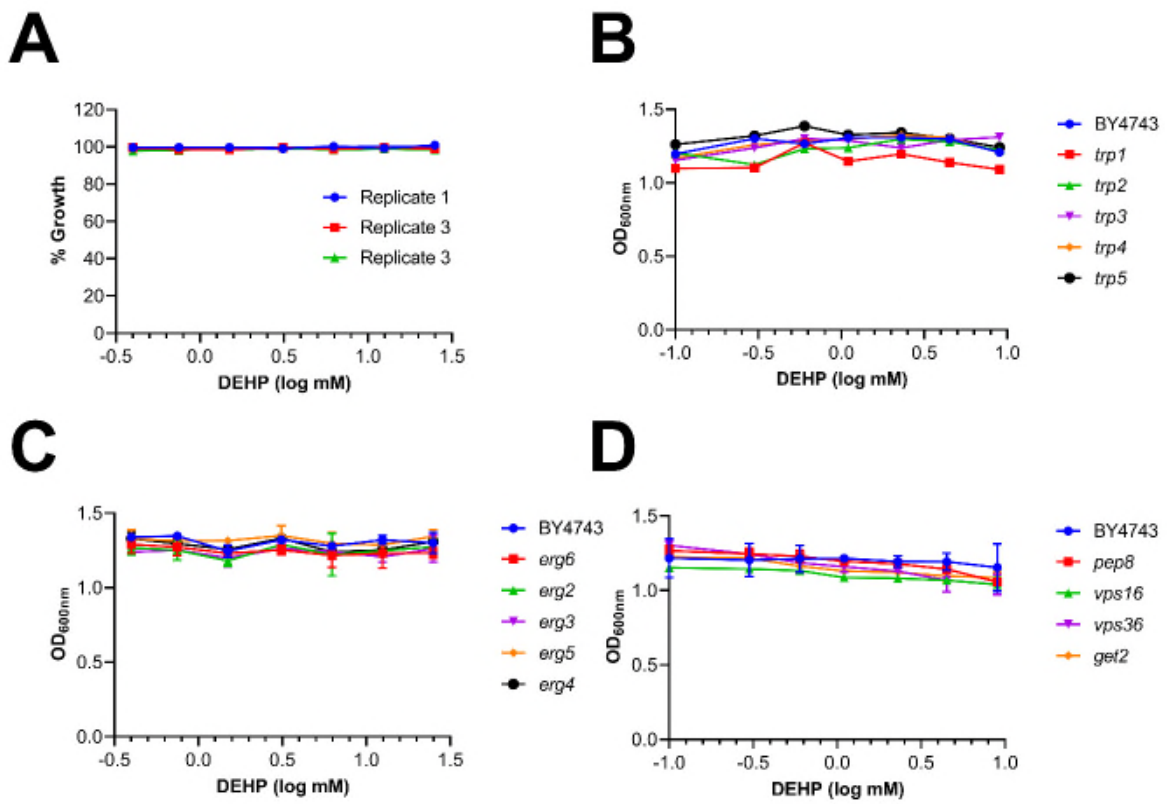

Supplementary fig. 1. Effect of DEHP on the growth of *Saccharomyces cerevisiae*.

A. Inhibitory Concentration (IC) of DEHP was determined for *Saccharomyces cerevisiae* strain (BY4743). Cells were incubated with various concentrations DEHP in YPD-HEPES (YPD + 25 mM HEPES, pH=6.8) medium at 30°C. Experiments were performed with triplicates in 96-well microplate. Growth of the cells was quantified by measuring the OD_{600nm} after 24 hours. Growth is plotted against concentration of the compound.

B. Wild type strain (BY4743) and tryptophan biosynthetic mutants (*trp1*, *trp2*, *trp3*, *trp4* and *trp5*) were grown in YPD-HEPES (YPD + 25 mM HEPES, pH=6.8) medium at 30°C in the presence of indicated concentrations of DEHP. Growth was performed in the similar way as described in Fig. 3 and analyzed as supplementary fig. 1A.

C. Wild type strain (BY4743) and ergosterol biosynthetic mutants (*erg6*, *erg2*, *erg3*, *erg5* and *erg4*) were grown in YPD-HEPES (YPD + 25 mM HEPES, pH=6.8) medium at 30°C in the presence of indicated concentrations of DEHP. Growth was performed in the similar way as described in Fig. 4 and analyzed as supplementary fig.1A.

D. Wild type strain (BY4743) and cellular transport mutants (*pep8*, *vps16*, *vps36* and *get2*) were grown in YPD-HEPES (YPD + 25 mM HEPES, pH=6.8) medium at 30°C in the presence of indicated concentrations of DEHP. Growth was performed and in the similar way as described in Fig. 5 and analyzed as supplementary fig. 1A.

A

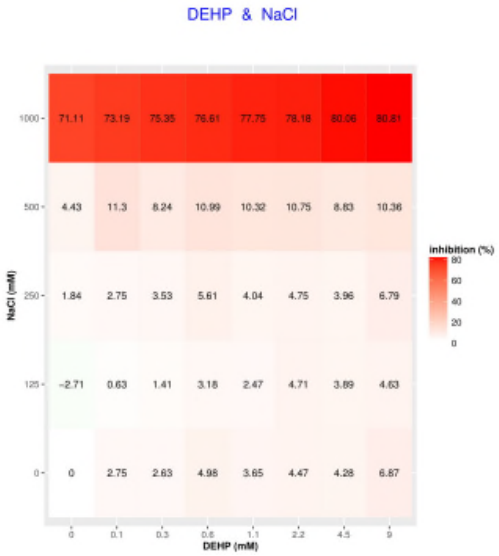
DEHP & NaCl
NaCl (mM)
DEHP (mM)
inhibition (%)

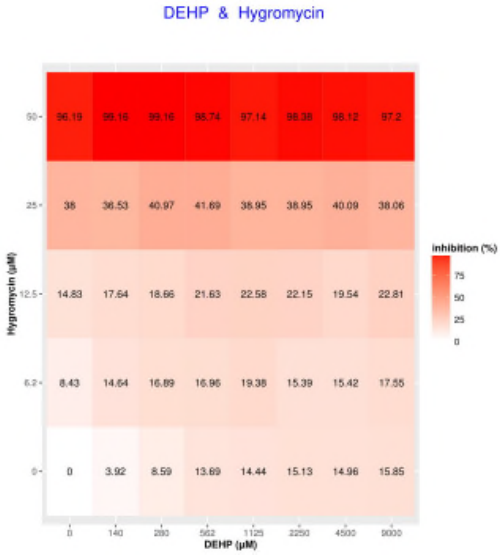
DEHP & Hygromycin
Hygromycin (μM)
DEHP (μM)
inhibition (%)

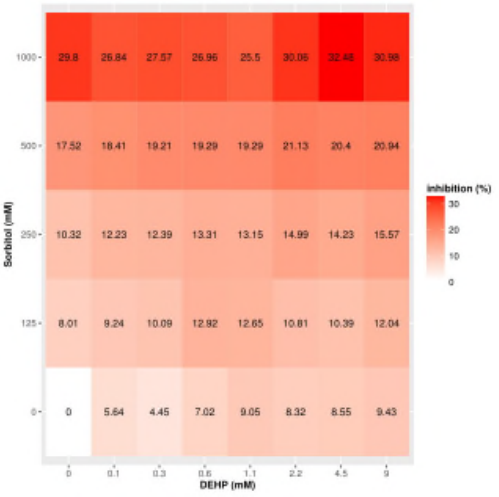
DEHP & Sorbitol
Sorbitol (mM)
DEHP (mM)
inhibition (%)

B

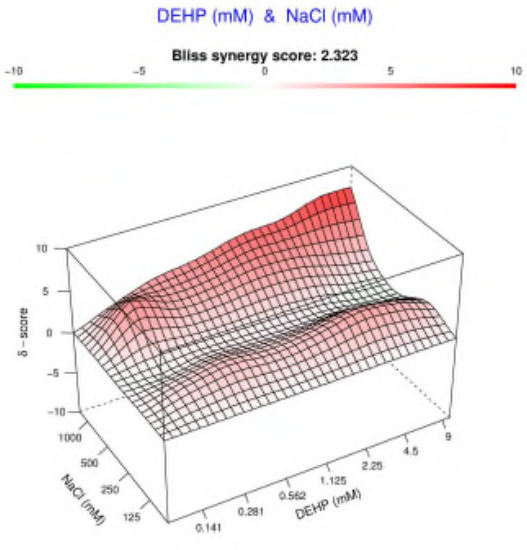
DEHP (mM) & NaCl (mM)
Bliss synergy score: 2.323
δ – score
NaCl (mM)
DEHP (mM)

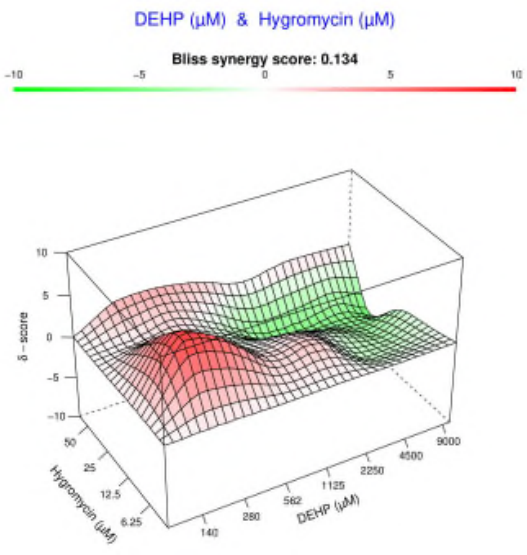
DEHP (μM) & Hygromycin (μM)
Bliss synergy score: 0.134
δ – score
Hygromycin (μM)
DEHP (μM)

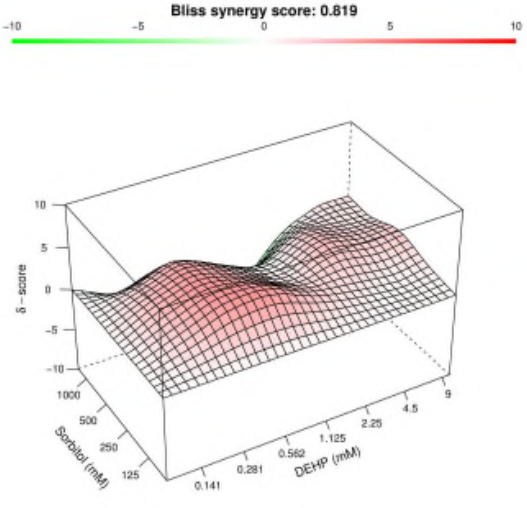
DEHP (mM) & Sorbitol (mM)
Bliss synergy score: 0.819
δ – score
Sorbitol (mM)
DEHP (mM)

Supplementary fig. 2. DEHP does not induce ionic and osmotic stress in yeast cells.

Wild type strain (BY4743) was grown in YPD-HEPES (YPD + 25 mM HEPES, pH=6.8) medium at 30°C in the presence of indicated concentrations of DEHP and NaCl or hygromycin or sorbitol. Growth at the different concentrations was recorded after 24 hours. Growth was performed and analyzed in the similar way as described in Fig. 6. Dose−response matrix (% growth inhibition) (supplementary fig. 2A) and their corresponding Bliss synergy scores visualized by 3D synergy map (supplementary fig. 2B). Two independent experiments were performed.

A

Amphotericin B & DEHP

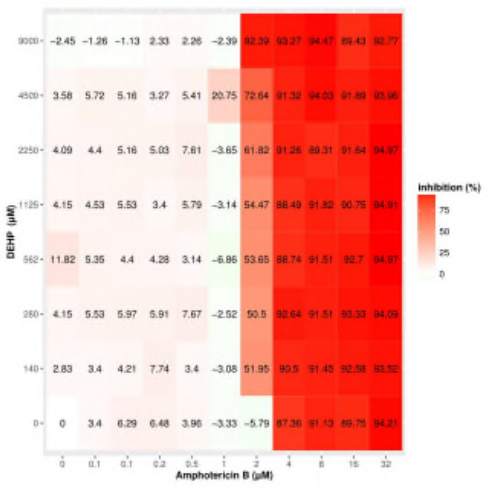

Dihydrosphingosine & DEHP

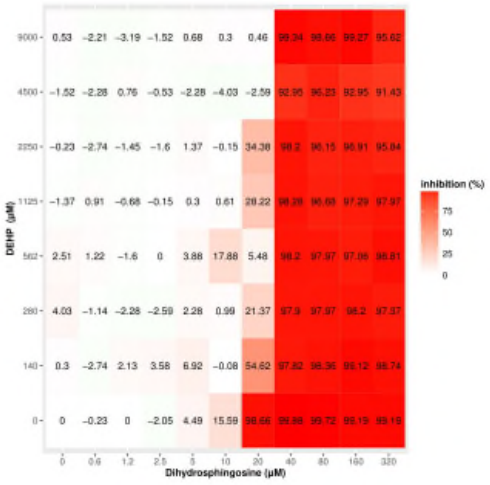

Phytosphingosine & DEHP

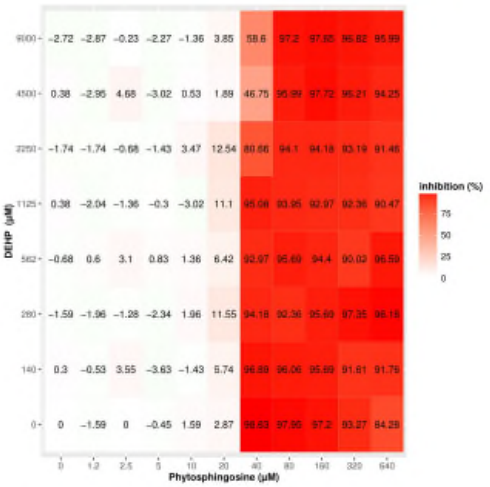

B

Amphotericin B (μM) & DEHP (μM)

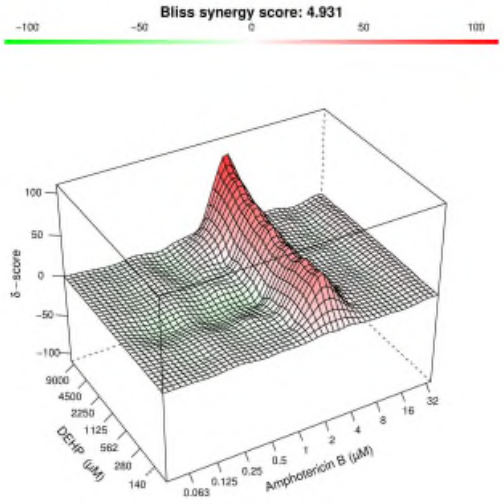

Dihydrosphingosine (μM) & DEHP (μM)

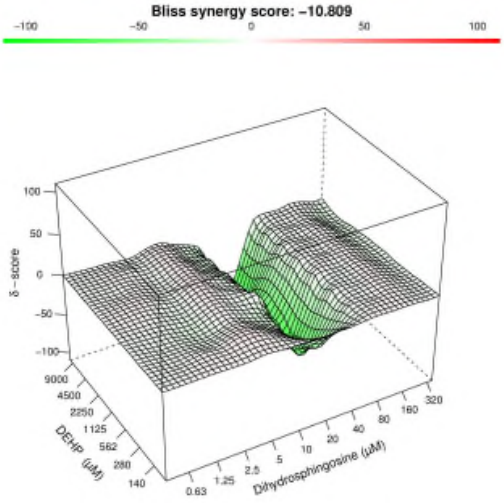

Phytosphingosine (μM) & DEHP (μM)

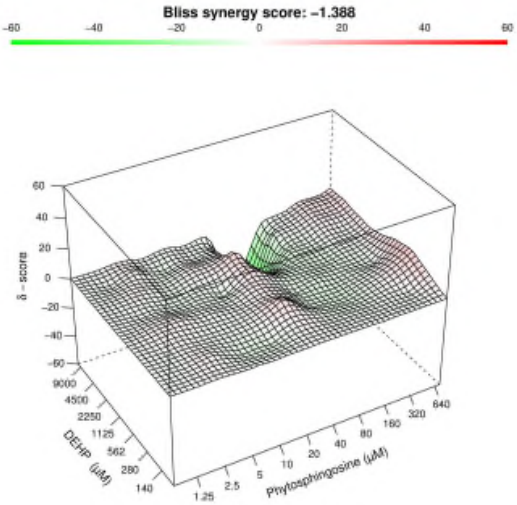

Supplementary fig. 3. DEHP does not interact with the membrane perturbing agent amphotericin B, dihydrosphingosine and phytosphingosine

Wild type strain (BY4743) were grown in YPD-HEPES (YPD + 25 mM HEPES, pH=6.8) medium at 30°C in the presence of indicated concentrations of DEHP and amphotericin B or dihydrosphingosine or phytosphingosine. Growth of cells was analyzed in the similar way as described in fig. 7. Dose−response matrix (% growth inhibition) (supplementary fig. 3A) and their corresponding Bliss synergy scores visualized by 3D synergy map (supplementary fig. 3B). Two independent experiments were performed.